THE ASTROPHYSICAL JOURNAL, 302:120–137, 1986 March 1


# WAVE PROPAGATION IN PULSAR MAGNETOSPHERES: DISPERSION RELATIONS AND NORMAL MODES OF PLASMAS IN SUPERSTRONG MAGNETIC FIELDS

JONATHAN ARONS
Department of Astronomy and Department of Physics, University of California at Berkeley, and Institute of Geophysics and Planetary Physics, University of California, Lawrence Livermore National Laboratory

AND

JOHN J. BARNARD[1]
Department of Astronomy, University of California at Berkeley, and Laboratory for High Energy Astrophysics, NASA-Goddard Space Flight Center
*Received 1985 April 5; accepted 1985 July 18*

## ABSTRACT

We derive the dispersion relations and polarization characteristics of the normal modes of radiation in superstrong magnetic fields, with particular attention to those attributes of importance to the transfer of radiation in the relativistic electron-positron plasmas expected to occur in the magnetospheres of radio pulsars. We restrict ourselves to the regions where the proper frequency of cyclotron resonance greatly exceeds the proper frequencies of the radiative normal modes. The normal modes are derived when the plasma has no momentum dispersion across the magnetic field but has arbitrary momentum dispersion along the field. The contribution of displacement current to the propagation of these "hydromagnetic" waves is consistently included. The distinction between superluminous and subluminous modes is made in the superstrong regime, where drift motions across the field are negligible, and useful formulae for the Landau damping of the subluminous branch of ordinary mode (the Alfvén wave) are derived. These are used to set observational constraints on the geometry of the emission zone in radio pulsars, if the emission mechanism generates radiation in the form of subluminous waves. A brief discussion is given of the relevance of nonvacuum propagation to Razin suppression of bunched coherent curvature emission.

*Subject headings:* hydromagnetics — polarization — pulsars — radiation mechanisms

## I. INTRODUCTION

Radio pulsars and X-ray pulsars are assumed to be magnetized neutron stars with superstrong magnetic fields, $B_{\rm surface} \gtrsim 10^{12}$ gauss. In both cases, the basic evidence supporting this hypothesis comes from the application of theories of electromagnetic torque applied to the observed pulsation (Ostriker and Gunn 1969; Goldreich and Julian 1969; Pringle and Rees 1972; Baan and Treves 1973; Davidson and Ostriker 1973; Lamb, Pethick, and Pines 1973; Rappaport and Joss 1977; Mason 1977; Ghosh and Lamb 1979*a*, *b*; Arons and Lea 1980; Lamb 1984; Arons, McKee, and Pudritz 1986). In two X-ray pulsars, spectral features have been qualitatively identified with cyclotron line radiation in magnetic fields exceeding $10^{12}$ gauss (Trümper *et al.* 1978; Gruber *et al.* 1980; Voges *et al.* 1982). Detailed interpretations of the spectra and pulse shapes of both classes of objects have remained elusive, however, in part because the physics of radiation generation and transfer in superstrong magnetic fields is relatively undeveloped compared to what is known about radiation in unmagnetized and weakly magnetized plasmas. In the case of X-ray pulsars, the basic power source is accretion, and this leads to plasma conditions in which radiation transfer effects play a dominant role in the formation of the emergent spectrum (e.g., Mészáros 1984, and references therein). In radio pulsars, the power supply is rotation, but this fails to specify the plasma conditions with anything like the uniqueness of the accretion model. In the most developed magnetospheric models, the plasma supply occurs in the form of a relativistic, electron-positron plasma streaming away from the magnetic polar regions and other zones of the magnetosphere (Sturrock 1971; Ruderman and Sutherland 1975; Cheng, Ruderman, and Sutherland 1976; Arons and Scharlemann 1979; Arons 1981*a*, 1983*a*, *b*, 1984; Lominadze, Machabelli, and Usov 1983), with many suggestions of possible radiation emission mechanisms which might occur in such plasmas (see Michel 1982 for a summary of most of these). There have also been suggestions that many of the observed phenomena might be due to transfer effects in such relativistic plasmas (e.g., Cordes and Hankins 1977; Harding and Tademaru 1979; Arons 1979; Cheng and Ruderman 1979; Melrose and Stoneham 1977; Melrose 1979; Arons 1981*b*; Onischenko 1981). A quantitative consideration of these requires a detailed knowledge of the propagation characteristics of the radiation normal modes in such plasmas.

Previous authors have investigated some aspects of propagation in pulsar plasmas. Tsytovitch and Kaplan (1972) derived the dispersion relation for a one-dimensional plasma with a power-law distribution function in an infinitely strong magnetic field, with vacuum polarizability neglected. Melrose and Stoneham (1977) included quantum effects and evaluated the dispersion relations in the "low-density" limit, appropriate when the departure of the index of refraction from unity is small. Others have addressed specific mechanisms for the formation of the orthogonal radiation modes observed in pulsar radio emission (e.g., Cheng and Ruderman 1979; Melrose 1979; Stinebring *et al.* 1984*a*, *b*); we provide a new interpretation of these phenomena in the accompany-

[1] Research Associate of the National Research Council.

ing paper (Barnard and Arons 1986, hereafter Paper II). In this paper, we reinvestigate the structure of the linear normal modes in pulsar plasmas (see Lominadze and Pataraya 1982 for some related work). Our investigation is oriented specifically toward putting the theory of the normal modes into a form useful for further studies of radiation transfer in these magnetospheres. Toward this end, we have incorporated a number of new features, allowing for finite charge and current density, as well as finding a number of useful expressions for the index of refraction in the strong field limit and deriving an expression for the Landau damping of subluminous waves with a component of the wave electric field along the magnetic field. Our primary interest is in the relativistic electron-positron plasma expected in the radio pulsar environment.

The plan of the paper is as follows. In § II, we derive the basic dispersion relation, assuming finite but strong magnetic field, in the small Larmor radius approximation appropriate to the interior regions or pulsar magnetospheres. We also give general expressions for the polarization states of the waves which show how nonzero charge and current density lead to the normal modes being elliptically polarized, even in superstrong magnetic fields. We then turn to the specific characteristics of the extraordinary mode (variously known as the $X$-mode, the $E$-mode, and the fast magnetosonic mode), where we show that it decouples from the plasma as the magnetic field strength becomes sufficiently strong. The detailed characteristics of the ordinary mode are described in § III, including its separation into subluminous (Alfvén wave) and superluminous (the fast mode) branches, and separation into high- and low-density propagation characteristics as a function of propagation direction in a relativistic plasma. In § IV, we calculate the damping decrement of the Alfvén wave (the subluminous $O$-mode), and contrast the results of the theory of hydromagnetic wave damping derived here with nonzero plasma frequency to previous studies in which the plasma frequency is taken to be infinite but the perpendicular velocity dispersion is assumed to be substantial. We solve the $X$-mode dispersion relation with nonzero ratio of the plasma energy density to the magnetic energy density in § V. Our results are summarized and their relevance to pulsar phenomenology outlined qualitatively in § VI.

## II. DISPERSION RELATIONS

### a) *General Theory of the Mobility Tensor for a Uniform Relativistic Plasma in a Uniform Magnetic Field*

We consider the propagation of electromagnetic waves in a plasma which can be ultrarelativistically streaming and can have ultrarelativistic momentum dispersion. We assume the wavelengths to be small compared to the scale lengths of the plasma and of the magnetic field in which the plasma is immersed. Let $F_s(\boldsymbol{u})$ be the locally homogeneous distribution function of species $s$ in the absence of the waves, normalized to unity. Here $\boldsymbol{u} = \boldsymbol{p}/m_s c$ is the spacelike part of the four-velocity of a particle of species $s$, while $\boldsymbol{p}$ is the momentum, $m_s$ the rest mass, and $c$ the speed of light. We take the Fourier transform of the Vlasov-Maxwell equations, assuming the fields are slowly switched on from time $= -\infty$. This assures us that the fields satisfy causality (Baldwin, Bernstein, and Weenink 1969), and it yields dispersion relations defined for $\mathrm{Im}(\omega) > 0$, where Fourier transforms are assumed to be proportional to $\exp\,[i(\boldsymbol{k}\cdot\boldsymbol{r} - \omega t)]$. Solutions for $\mathrm{Im}(\omega) \le 0$ are obtained by analytic continuation. After inclusion of the vacuum polarization effects following the work of Kirk (1980), we find the transformed wave equation

$$\{[(k^2c^2 - \omega^2)\delta_{ij} - k_i k_j c^2]a + M_{ij} - \omega^2 Q\delta_{i3}\delta_{j3} - c^2k_\perp^2 R\delta_{i2}\delta_{j2}\}\delta\hat{E}_j = 0\,, \tag{1}$$

where $i, j = x, y, z$, with the $z$-axis aligned parallel to the locally homogeneous magnetic field, the $x$-axis orientated so that the wave vector $\boldsymbol{k}$ lies in the $(x, z)$-plane at an angle $\theta$ the $\boldsymbol{B}$ field, $a = 1 - 2b$, $Q = 7b$, $R = 4b$,

$$b = \frac{\alpha_F}{45\pi}\left(\frac{B}{B_c}\right)^2 = \frac{\alpha_F}{45\pi}\left(\frac{\hbar\omega_{ce}}{m_e c^2}\right)^2\,, \tag{2}$$

$\alpha_F$ is the fine structure constant, $\omega_{ce} = eB/m_e c$ is the nonrelativistic cyclotron frequency, $\delta\hat{E}(\boldsymbol{k}, \omega)$ is the Fourier transform of the wave electric field, and $M_{ij}(\boldsymbol{k}, \omega) = \sum_s M_{ijs}(\boldsymbol{k}, \omega)$ is the mobility tensor of the plasma. For a given electric field component $\delta\hat{E}_i(\boldsymbol{k}, \omega)$, the mobility tensor is defined by

$$\delta\hat{J}_i(\boldsymbol{k}, \omega) = (i/4\pi\omega)M_{ij}(\boldsymbol{k}, \omega)\delta\hat{E}_j(\boldsymbol{k}, \omega)\,, \tag{3}$$

where $\delta\boldsymbol{J}$ is the current induced in the plasma by the electric field. The summation convention on repeated indices is understood in expressions such as equation (3).

Standard methods (Baldwin, Bernstein, and Weenink 1969; Barnes and Scargle 1973) yield

$$M_{ijs} = -2\pi\omega_{ps}^2\int_0^\infty du_\perp u_\perp^2\int_{-\infty}^\infty du_\parallel\left[(\omega - ck_\parallel\beta_\parallel)\frac{\partial F_s}{\partial u_\perp} + k_\parallel c\beta_\perp\frac{\partial F_s}{\partial u_\parallel}\right]\Phi_{ijs} - 2\pi\omega_{ps}^2\int_0^\infty du_\perp\int_{-\infty}^\infty du_\parallel u_\parallel\beta_\perp\frac{\partial F_s}{\partial u_\parallel} - \beta_\parallel\frac{\partial F_s}{\partial u_\perp}\delta_{i3}\delta_{j3}\,, \tag{4}$$

with

$$\Phi_{ijs} = \sum_{n=-\infty}^{\infty} T_{ijs}^{(n)}\Big/[\gamma(\omega - ck_\parallel\beta_\parallel) - n\omega_{cs}]\,, \tag{5}$$

and

$$T_{ijs}^{(n)} = \begin{bmatrix} \frac{n^2}{z_s^2} J_n^2(z_s) & \frac{in}{z_s} J_n(z_s)J_n'(z_s) & \frac{nu_\parallel}{z_s u_\perp} J_n^2(z_s) \\ -\frac{in}{z_s} J_n(z_s)J_n'(z_s) & [J_n'(z_s)]^2 & -\frac{iu_\parallel}{u_\perp} J_n(z_s)J_n'(z_s) \\ \frac{nu_\parallel}{z_s u_\perp} J_n^2(z_s) & \frac{iu_\parallel}{u_\perp} J_n(z_s)J_n'(z_s) & \left(\frac{u_\parallel}{u_\perp}\right)^2 J_n^2(z_s) \end{bmatrix} . \tag{6}$$

Here $\gamma = (1 + u^2)^{1/2}$, $\beta = u/\gamma$, $z_s = k_\perp c u_\perp/\omega_{cs}$, $\omega_{cs} = q_s B/m_s c$, and $k_\perp$, $k_\parallel$ are the magnitudes of the components of $\boldsymbol{k}$ perpendicular and parallel to $B$, respectively, with similar interpretation for $u_\perp$ and $u_\parallel$.

We are interested in the wave propagation characteristics of plasmas with Larmor radii small compared to the wavelengths of the normal modes; in fact, under conditions thought to be typical in pulsar magnetospheres, the particles may be all in their lowest Landau level, with no Larmor gyration whatsoever, while still having relativistic momentum dispersion along the magnetic field. This is because the synchrotron loss time for the decay of the perpendicular momentum of an electron (or positron) is $\sim 10^{-17}$ $(100/\gamma)(10^{+12}$ gauss$/B) \sin^{-2} \psi$ s, where $\psi = \sin^{-1}(u_\perp/u)$ is the pitch angle. Since a particle with nonzero gyrational momentum has pitch angle exceeding $(2\hbar\omega_c/mc^2\gamma^2)^{1/2}$, the synchrotron loss time is always less than $3 \times 10^{-14}(\gamma/100)$ $(10^{12}$ gauss$/B)^2$ s, a result obtained by transforming the cyclotron decay time from the lowest Landau level back into the laboratory from the frame where the particle's pitch angle is 90°. This time is always short compared to the transit time at the stellar surface for any velocity. Most plasma supply models for either radio or X-ray pulsars therefore predict one-dimensional distributions of random momenta, with all momentum dispersion along $B$. Pitch angle scattering at large radii may reduce this anisotropy (Benford 1975; Lominadze, Machabelli, and Usov 1983); for now, we neglect this possibility and consider only the radiative decayed case. Then it is useful to expand the matrix in equation (5) to lowest significant order in $z$, which yields

$$\Phi_{ijs} = \frac{T_{ijs}^{(0)}}{\gamma(\omega - ck_\parallel \beta_\parallel)} + \frac{T_{ijs}^{(+)}}{\gamma(\omega - ck_\parallel \beta_\parallel) - \omega_{cs}} + \frac{T_{ijs}^{(-)}}{\gamma(\omega - ck_\parallel \beta_\parallel) + \omega_{cs}} , \tag{7}$$

with

$$T_{ijs}^{(0)} = \begin{bmatrix} 0 & 0 & 0 \\ 0 & \frac{z_s^2}{4} & \frac{iu_\parallel z_s}{2u_\perp} \\ 0 & -\frac{iu_\parallel}{2u_\perp} & \frac{u_\parallel^2}{u_\perp}\left(1 - \frac{z_s^2}{z}\right) \end{bmatrix} , \tag{8}$$

and

$$T_{ijs}^{(\pm)} = \frac{1}{4} \begin{bmatrix} 1 & \pm i & \pm u_\parallel z_s/u_\perp \\ \mp i & 1 & -iu_\parallel z_s/u_\perp \\ \pm u_\parallel z_s/u_\perp & iu_\parallel z_s/u_\perp & u_\parallel^2 z_s^2/u_\perp^2 \end{bmatrix} . \tag{9}$$

For a large number of applications to radiation propagation in the inner magnetosphere, the cyclotron frequencies are large compared to the Doppler shifted wave frequencies. Therefore, we assume $|\omega_{cs}| \gg \gamma(\omega - k_\parallel c\beta_\parallel)$, and also assume negligible dispersion in the perpendicular momenta by writing

$$F_s = \frac{1}{2\pi u_\perp} \delta(u_\perp) f_s(u_\parallel) . \tag{10}$$

Integration over all $u_\perp$ yields the mobility tensors, whose components are

$$M_{11s} = M_{22s} = \frac{4\pi}{B^2} (\omega^2 U_s + k_\parallel^2 c^2 P_{\parallel s} - 2\omega c k_\parallel c \Pi_s) , \tag{11}$$

$$M_{33s} = -\frac{\omega^2 \omega_{ps}^2}{ck_\parallel} \int_{-\infty}^{\infty} \frac{du_\parallel f_s'(u_\parallel)}{\omega - ck_\parallel \beta_\parallel} + \frac{1}{2} \frac{c^2 k_\perp^2}{\omega_{cs}^2} \omega_{ps}^2 \langle \gamma \beta_\parallel^2 \rangle_s , \tag{12}$$

$$M_{12s} = -M_{21s} = \frac{4\pi i q_s n_s c}{B} (\omega - k_\parallel c \langle \beta_\parallel \rangle_s) , \tag{13}$$

$$M_{23s} = -M_{32s} = \frac{4\pi i c k_\perp q_s n_s c}{B} \langle \beta_\parallel \rangle_s \tag{14}$$

and

$$M_{13s} = M_{31s} = \frac{4\pi k_\perp k_\parallel c^2}{B^2}\left(P_{\parallel s} - \frac{\omega}{k_\parallel}\Pi_s\right). \tag{15}$$

Here

$$c\langle\beta_\parallel\rangle_s = c\int_{-\infty}^{\infty} du_\parallel\, \beta_\parallel f_s(u_\parallel) \tag{16}$$

is the average streaming speed of the $s$th component of the plasma along $B$,

$$U_s = n_s m_s c^2 \int_{-\infty}^{\infty} du_\parallel\, \gamma f_s(u_\parallel) = \langle\gamma\rangle_s n_s m_s c^2 \tag{17}$$

is the energy density (including rest energy) of the $s$th component,

$$\Pi_s = n_s m_s c \int_{-\infty}^{\infty} du_\parallel\, u_\parallel f_s(u_\parallel) = n_s m_s c\langle\beta_\parallel \gamma\rangle_s \tag{18}$$

is the momentum density of the $s$th component, and

$$P_{\parallel s} = n_s m_s c^2 \int_{-\infty}^{\infty} du_\parallel\, \beta_\parallel u_\parallel f_s(u_\parallel) = n_s m_s c^2\langle\beta_\parallel^2 \gamma\rangle_s \tag{19}$$

is the parallel pressure in the $s$th component. The density $n_s$ is that measured in the reference frame where the distribution function has the form (10). For our purposes, this corresponds *extremely* closely to the frame corotating with the neutron star, since the macroscopic electric field in the plasmas of interest differs only slightly from the corotation field, and other cross field drifts are negligible, for plasma motion well inside the light cylinder.

### b) *Particle Model of the Mobility Tensor*

It is informative to use a simple particle model to interpret the physical content of the mobility tensor for these low-frequency waves. Consider a particle moving with speed $c\beta_s$ along $B$. The linearized response of each particle's four-velocity to the wave electromagnetic field is described by the momentum equation

$$\frac{\partial \delta \boldsymbol{u}}{\partial t} + c\beta_s \frac{\partial \delta \boldsymbol{u}}{\partial z} = \frac{q_s}{m_s c}(\delta \boldsymbol{E} + \beta_s \boldsymbol{b} \times \delta \boldsymbol{B} + \delta \boldsymbol{\beta}_\perp \times \boldsymbol{b}B). \tag{20}$$

Now compute the perpendicular velocity, for which $\delta \boldsymbol{u}_\perp = \gamma_s \delta\boldsymbol{\beta}_\perp$. After taking the Fourier transform and vector multiplying by $\boldsymbol{B}$, we find

$$\delta\boldsymbol{\beta}_{s\perp} = \frac{\delta \boldsymbol{E}_\perp \times \boldsymbol{b}}{B} + \beta_s \frac{\delta \boldsymbol{\beta}_\perp}{B} - i\,\frac{\gamma_s(\omega - ck_\parallel \beta_s)}{\omega_{cs}}\, \boldsymbol{b} \times \delta\boldsymbol{\beta}_{s\perp}. \tag{21}$$

Since we are interested in Doppler-shifted frequencies low compared to the cyclotron frequency, we solve equation (21) for $\delta\boldsymbol{\beta}_{s\perp}$ through first and second order in $B^{-1}$ by substituting the first two terms into the third. This yields

$$\delta\boldsymbol{\beta}_{s\perp} = \frac{\delta \boldsymbol{E}_\perp \times \boldsymbol{b}}{B} + \beta_s \frac{\delta \boldsymbol{\beta}_\perp}{B} - i\,\frac{\gamma_s(\omega - ck_\parallel \beta_s)}{\omega_{cs}}(\delta \boldsymbol{E}_\perp + \beta_s \boldsymbol{b} \times \delta \boldsymbol{B}_\perp). \tag{22}$$

The first term is recognizable as the $\boldsymbol{E} \times \boldsymbol{B}$ drift in a low-frequency electric field. The second is the drift due to the $(\boldsymbol{v}_s \times \delta\boldsymbol{B}) \times \boldsymbol{B}$ drift, while the third is the inertial ("polarization") drift, due to the finite inertia of the particle.

We now use Faraday's law to express $\delta\boldsymbol{B}$ in terms of $\delta\boldsymbol{E}$, with $\boldsymbol{k}$ in the $(x - z)$-plane; this defines the $x$-axis. Then

$$\delta\beta_{sx} = \frac{\delta E_y}{B}(1 - n_\parallel \beta_s) - i\,\frac{\omega\gamma_s}{\omega_{cs}}(1 - n_\parallel\beta_s)^2 \frac{\delta E_x}{B} - in_\perp \beta_s \gamma_s(1 - n_\parallel \beta_s)\frac{\omega}{\omega_{cs}}\frac{\delta E_\parallel}{B}, \tag{23}$$

and

$$\delta\beta_{sy} = -\frac{\delta E_x}{B}(1 - n_\parallel \beta_s) - \frac{i\omega}{\omega_{cs}}\gamma_s(1 - n_\parallel\beta_s)^2 \frac{\delta E_y}{B} - n_\perp \beta_s \frac{\delta E_\parallel}{B}. \tag{24}$$

Here $n_\parallel = ck_\parallel/\omega$ and $n_\perp = ck_\perp/\omega$ are the parallel and perpendicular components of the refractive index. For propagation almost along $\boldsymbol{\beta}_s$ and $\boldsymbol{B}$, the $(\boldsymbol{v}_s \times \delta\boldsymbol{B}) \times \boldsymbol{B}$ drift almost cancels the $\delta\boldsymbol{E} \times \boldsymbol{B}$ drift. This greatly reduces the polarization drift since this is now proportional to the Doppler-shifted frequency times the total Lorentz force drift, which is itself proportional to the Doppler-shifted frequency.

Now compute the current due to all the particles with velocity $c\boldsymbol{\beta}_s$. The component perpendicular to the plane of $k$ and $B$ is

$$\delta J_{ys}(\beta_s) = -\frac{q_s n_s c}{B}(1 - n_\parallel \beta_s)\delta E_x - i\,\frac{\omega}{\omega_{cs}}\, n_s q_s \gamma_s c(1 - n_\parallel\beta_s)^2 \delta E_y - n_\perp q_s n_s c\beta_s\left(\frac{\delta E_\parallel}{B}\right). \tag{25}$$

Comparison to equation (3) yields

$$M_{21s} = -M_{12s} = \frac{4\pi i q_s n_s c\omega}{B}(1 - n_\parallel \beta_\parallel) ,$$

$$M_{22s} = -\frac{4\pi\omega^2}{B^2}\gamma_s n_s m_s c^2(1 - 2n_\parallel \beta_\parallel + n_\parallel^2 \beta_\parallel^2) , \tag{26}$$

$$M_{23s} = -M_{32s} = \frac{4\pi i k_\perp c q_s n_s c}{B}\beta_\parallel ,$$

for the mobility of the particles with velocity $c\beta_\parallel$ which contribute to the current in the $y$-direction. Summation over all speeds yields the forms found in the formal theory; in particular, $M_{22}$ is seen to be the result of the inertial drift in the plasma, with the dependence on energy density being the same as in the cold plasma theory, while the contribution of the momentum density and the parallel pressure comes entirely from the fully electromagnetic, $(\boldsymbol{v}_s \times \delta\boldsymbol{B}) \times \boldsymbol{B}$ part of the Lorentz force contribution to the inertial drift. The quantity $M_{21}$ represents the contribution of Lorentz force times the $B$ drift, modified substantially from the cold plasma $\delta\boldsymbol{E} \times \boldsymbol{B}$ drift result only when the velocities are relativistic. Since the plasma has no perpendicular momentum dispersion, $M_{23} \neq 0$ only because of the $(\boldsymbol{v}_s \times \delta\boldsymbol{B}) \times \boldsymbol{B}$ drift, which creates a current in the $y$-direction from any $\delta E_\perp$. This contrasts to the coupling created by the magnetic mirror force when the particles have finite Larmor radii (e.g., Barnes 1966); this coupling is negligible in the inner magnetospheres of pulsars, at least for electrons and positrons, but may be of significance in the outer magnetosphere where strong pitch angle scattering may occur (e.g., Benford 1975; Hardee 1979; Lominadze, Machabelli, and Usov 1983). We analyze this possibility elsewhere. Similar analysis provides the analogous interpretation of $M_{13}$, $M_{31}$, and $M_{11}$.

The parallel mobility (eq. [12]) has two parts. The second term, proportional to $B^{-2}$, can be derived from a fluid model. In response to a perturbed velocity $\delta v_s$, the plasma acquires a density disturbance $\delta n_s$. The advection of this density disturbance creates a perturbed current $q_s c\beta_s \delta n_s$ along $B$. The continuity equation yields

$$\frac{\delta n_s}{n_s} = (1 - n_\parallel \beta_s)^{-1}(n_\parallel \delta\beta_{s\parallel} + n_\perp \delta\beta_{sx}) . \tag{27}$$

Inspection of equation (22) reveals a term proportional to $\delta E_\parallel$, arising from the magnetic part of the Lorentz force times the $B$ drift. Upon using this in equation (27) and using the result in the part of the parallel current due to advection of $\delta n_s$, we obtain the second term in equation (12). Therefore, this part of the parallel response comes from perpendicular motion across $B$, induced by the $(\boldsymbol{v}_s \times \delta\boldsymbol{B}) \times \boldsymbol{B}$ drift, which derives from $\delta E_\parallel$ since this component of $\delta\boldsymbol{E}$ induces a $\delta\boldsymbol{B}_\perp$ when $\boldsymbol{k}$ is not along $B$.

The first part of $M_{33}$ contains the Landau resonant response of the plasma. This is not derivable from a fluid model, but can be obtained from the Vlasov equation in which only velocities and momenta parallel to $B$ are retained; the full result for $M_{33}$ is found if the particle drifts across $B$ are kept in the advection term. This is equivalent to the formal theory given above. The physical interpretation of the resonance is the same as in the nonrelativistic theory; see Dawson (1961), for example, for a derivation of the resonant energy exchange when the waves are subluminous, i.e., have phase velocities less than the speed of light.

### c) *Dispersion Relations*

We now sum over species in equations (11)–(15), to find

$$M_{11} = M_{22} = -\frac{4\pi\omega^2}{B^2}(U - 2n_\parallel c\Pi + n_\parallel^2 P_\parallel) , \tag{28}$$

$$M_{12} = -M_{21} = -\frac{4\pi i\omega}{B}(c\eta - n_\parallel J_\parallel) , \tag{29}$$

$$M_{13} = M_{31} = \frac{4\pi\omega^2}{B^2} n_\perp(n_\parallel P_\parallel - c\Pi) , \tag{30}$$

$$M_{23} = -M_{32} = \frac{4\pi i\omega}{B} n_\perp J_\parallel , \tag{31}$$

$$M_{33} = -\frac{1}{n_\parallel}\sum_s \omega_{ps}^2 \int_{-\infty}^{\infty} \frac{du_\parallel f_s'}{1 - n_\parallel \beta_\parallel} + \frac{1}{2}\omega^2 n_\perp^2 \frac{4\pi P_\parallel}{B^2} . \tag{32}$$

Here $U$ is the total energy density, $P_\parallel$ is the total parallel pressure, $\Pi$ is the total momentum density, $\eta$ is the charge density, $J_\parallel$ is the density of electric current flowing along $B$, $n_\parallel$ and $n_\perp$ are the components of the index of refraction parallel and perpendicular to the magnetic field, respectively, and $\omega_{ps}$ is the plasma frequency of the $s$th component.

It is useful to define

$$D_X = 1 + \frac{4\pi U}{aB^2}\left(1 - \frac{2c\Pi}{U} n_\parallel + \frac{P_\parallel}{U} n_\parallel^2\right) - n^2 , \tag{33}$$

and

$$D_A = D_X + n_\perp^2 \,. \tag{34}$$

The quantities $D_X + n^2$ and $D_A + n_\parallel^2$ are recognizable as the low-frequency dielectric function of a magnetized, uniform plasma, here generalized to include relativistic mass, momentum flow along $B$ and momentum dispersion along $B$, as well as vacuum polarization. We will also need

$$D_p = 1 + \frac{1}{a}(Q + 4\pi\chi_\parallel) - n_\perp^2 \,, \tag{35}$$

where $D_p + n_\parallel^2$ is the longitudinal dielectric function for response parallel to $B$ and $\chi_\parallel$ is the longitudinal susceptibility. From equations (3) and (32),

$$4\pi\chi_\parallel = \sum_s \frac{\omega_{ps}^2}{\omega^2 n_\parallel} \int_{-\infty}^{\infty} \frac{du_\parallel f_s'(u_\parallel)}{1 - n_\parallel \beta_\parallel} - \frac{1}{2} n_\perp^2 \frac{4\pi P_\parallel}{B^2} \,. \tag{36}$$

Finally, define

$$D_O = D_A D_p - \frac{n_\perp^2 n_\parallel^2}{a}\left[1 - 2b - \frac{4\pi}{B^2}\left(P_\parallel - \frac{c\Pi}{n_\parallel}\right)\right]^2 . \tag{37}$$

Then the wave equation (1) has a nontrivial solution if and only if the dispersion relation

$$D_X D_O = \frac{16\pi^2}{a^2\omega^2 B^2}\left[n_\perp^2 J_\parallel^2 D_A + (c\eta - n_\parallel J_\parallel)^2 D_p + n_\perp^2 n_\parallel \frac{(K - 2b)}{a} J_\parallel (c\eta - n_\parallel J_\parallel)(1 + a^{-1})\right] \tag{38}$$

is satisfied by all $\omega$, $k$. Here

$$K = 1 - \frac{4\pi}{B^2}\left(P_\parallel - \frac{c\Pi}{n_\parallel}\right) \tag{39}$$

The polarization states are obtained from the wave equation (1). We find

$$\frac{\delta E_y}{\delta E_x} = -\frac{4\pi i}{aB\omega} \frac{D_p(c\eta - n_\parallel J_\parallel) + n_\perp^2 n_\parallel (K - 2b) J_\parallel a^{-1}}{D_x D_p - 16\pi^2 n_\perp^2 J_\parallel^2 B^{-2} \omega^{-2} a^{-2}} \,, \tag{40}$$

and

$$\frac{\delta E_\parallel}{\delta E_x} = -\left[\frac{n_\perp}{a} \frac{n_\parallel (K - 2b) D_x + 16\pi^2 J_\parallel (c\eta - n_\parallel J_\parallel)(aB\omega)^{-2}}{D_x D_p - 16\pi^2 n_\perp^2 J_\parallel^2 (aB\omega)^{-2}}\right] , \tag{41}$$

where the $x$-component of $\delta \boldsymbol{E}$ lies in the $(\boldsymbol{k}, \boldsymbol{B})$-plane, and $\delta E_\parallel$ is the component of $\delta \boldsymbol{E}$ parallel to $\boldsymbol{B}$.

Expressions (40) and (41) show that in the general case, nonzero charge density and field-aligned current densities in the magnetosphere cause the normal modes to be elliptically polarized. Differences in the intertia of the species are another mechanism, hidden within equations (38)–(41), which can lead to elliptical polarization. The radiation which eventually emerges into the weakly magnetized universe exterior to the magnetosphere is known to be elliptically polarized in general (Stinebring *et al.* 1984*a*, *b*), although some cases of almost pure linear polarization do exist.

In the most commonly considered models of pulsar magnetospheres, the charge density is almost equal to the corotation value $\eta_R = -\boldsymbol{\Omega}_* \cdot \boldsymbol{B}/2\pi c$, where $\boldsymbol{\Omega}_*$ is the angular velocity of the star and $J_\parallel$ is usually assumed to be zero ("closed" field lines) or to be the Goldreich-Julian current density, $J_\parallel = B/Pc$. We point out that neither of these assumptions is necessarily true, especially if the emission and radiative transfer regions are in boundary layers between dense plasma zones and lower density "starvation" zones, or "gaps" (Arons 1981*a*, *b*, 1983*a*, *b*). In such boundary layers, much larger current and charge densities can occur, as well as strong differential acceleration between the species, all of which may contribute to the strong elliptical polarization observed in the emergent radiation. However, in this and the accompanying paper on refraction of radio waves in the polar zones of pulsars, we do assume that the charge and field-aligned current densities are on the order of the corotation and Goldreich-Julian values, respectively, primarily to allow us to isolate the effects of high density and propagation almost aligned with the magnetic field on the refractive characteristics of the magnetosphere and the relation of these effects to the frequency dependence of beaming morphology. Then all the terms on the right-hand side of equation (38) are $O[(\Omega_*/\omega)^2]$. Even for waves of frequency as low as 10 MHz and rotation rates as fast as 2 kHz, the corrections to the dispersion relation obtained by not setting the right-hand side of equation (38) equal to zero are only $\sim 10^{-8}$. The dispersion relation then factors, representing the propagation of two uncoupled modes, the extraordinary or $X$-mode, obtained by setting $D_X = 0$, and the ordinary or $O$-mode, obtained by setting $D_O = 0$. The terminology is from conventional magnetoionic theory, since these waves are the analog of the magnetoionic modes in the $QT$-$X$ approximation.

In these "normal" regions not associated with a boundary layer, the dispersion relation for the $X$-mode $D_X = 0$ yields $\delta E_x = 0$ and $\delta E_\parallel = 0$ through zeroth order in $\Omega_*/\omega$; the $X$-mode is linearly polarized, with the electric field perpendicular to the $(\boldsymbol{k}, \boldsymbol{B})$-plane and the wave magnetic field in the $(\boldsymbol{k}, \boldsymbol{B})$-plane.

The ordinary mode exhibits a more complex structure. We rewrite equation (37) in a more instructive form by defining the transverse susceptibility

$$\chi_{\perp} = \frac{1}{B^2}(U - 2cn_{\parallel}\Pi + n_{\parallel}^2 P_{\parallel}) . \tag{42}$$

Then the dispersion relation for the ordinary mode is

$$D_O = (1 + 4\pi\chi_{\perp} - n_{\parallel}^2)(1 + 4\pi\chi_{\parallel} - n_{\perp}^2) - (n_{\perp} n_{\parallel}/a)^2(K - 2b) = 0 , \tag{43}$$

with $\chi_{\parallel}$ defined in equation (36), $K$ in equation (39), $b$ in equation (5), and $a = 1 - 2b$. In the simple case of perpendicular or parallel propagation, the dispersion relation factors. When $n_{\perp} = 0$, we have $n^2 = 1 + 4\pi\chi_{\perp}$, the dispersion relation and polarization for an Alfvén wave propagating along $B$. For $n_{\parallel} = 0$, we have $n_{\perp}^2 = 1 + 4\pi\chi_{\parallel}$, the dispersion relation for an electromagnetic wave propagating across $B$ with the wave electric field polarized along $B$, so that the plasma response is "ordinary," as if the magnetic field were absent.

For frequencies well below all the plasma frequencies (as well as being well below the cyclotron frequencies of all the species), $|4\pi\chi_{\parallel}| \gg 1$ and the $O$-mode dispersion relation has the approximate form $n_{\parallel}^2 \approx 1 + 4\pi\chi_{\perp}$, the dispersion relation of the magnetohydrodynamic Alfvén wave at all angles of $k$ with respect to $B$, including the firehose destabilization by parallel pressure. The polarization of the $O$-mode in this magnetohydrodynamic limit is linear, with $\delta \boldsymbol{E}$ perpendicular to $B$, to lowest order in $(\omega/\omega_p)^2$, and lying in the plane of $k$ and $B$, while $B$ is also linearly polarized, lying perpendicular to the plane of $\boldsymbol{k}$ and $\boldsymbol{B}$. Therefore, to lowest significant order in $(\omega/\omega_p)^2$, the Alfvén wave has its Poynting flux and group velocity along $B$, even when displacement current dominates conduction current and the phase and group velocities are almost $c$. The origin of this result is in the low frequency compared to the plasma frequencies of all the species. Then the plasma is rapidly mobile along $\boldsymbol{B}$ and shorts out $\delta \boldsymbol{E}_{\parallel}$, while the strong magnetization limits the transverse motions to $\delta \boldsymbol{E} \times \boldsymbol{B}$ drifts and polarization drifts. This results in there being a component of $\delta \boldsymbol{E}$ along $\boldsymbol{k}$ but none along $\boldsymbol{B}$, which gives rise to the ducting of wave energy along $B$.

The $O$-mode dispersion relation for $n_{\perp} = 0$ also incorporates plasma oscillations, since $D_O = 0$ can be satisfied either by $n^2 = 1 + 4\pi\chi_{\perp}$ or by $1 + 4\pi\chi_{\parallel} = 0$. The properties of these are determined by the details of the distribution function, as discussed below.

### *d)* $B = \infty$ *Approximation*

We now restrict our attention to wave propagation under conditions thought to be appropriate to the magnetospheres of radio pulsars, in regions where the cyclotron frequencies are large compared to the wave frequencies. We further specialize to the plasma conditions found in models of the polar flux tubes, in which electron-positron pair creation in and above a surface "gap" or "starvation zone" provides a relativistically outflowing, relativistically hot plasma with number density large compared to the corotation density $B/Pce = 7 \times 10^{10}$ $(B/10^{12}$ gauss$)/P$ cm$^{-3}$ (Sturrock 1971; Tademaru 1973; Ruderman and Sutherland 1975; Cheng and Ruderman 1977; Arons and Scharlemann 1979; Arons 1983*b* and Arons 1986). In the more modern versions of these models, the distribution of outflowing momenta has zero momentum dispersion in the perpendicular momenta, but is broad band parallel to the magnetic field. Typically (Arons 1986), the pairs have $f_s(u)$ nonzero between a lower cutoff momentum $u_0 \approx 10$–$50$ and an upper cutoff $u_m \approx 10^3$–$10^4$. Below the lower cutoff and above the upper cutoff, the particle spectrum declines exponentially. Between the cutoffs, the spectrum is a power law with a break in the spectral index, with the power law being slightly steeper than $u^{-1.5}$ below a break energy typically about several hundred MeV, and very flat between the break energy and the upper cutoff. In addition, the plasma is penetrated by the very high energy beam accelerated near the surface, as well as having a lower density component of trapped particles flowing back from high altitude on some of the field lines. These conditions are typical of most of the polar flux tube, while at the boundaries, the response of the plasma to the strong electric fields of the neighboring vacuum zones can lead to very different average conditions.

In this paper, we will neglect all of the complications, and consider only the dense, outflowing pair plasma on a typical field line. We also assume that the electron and positron distribution functions on each field line remain identical at all altitudes. Furthermore, we replace the structure in $f_s(u)$ by simple model distributions. We allow the density and energy density to be free parameters, constrained only by the general limits found in the pair creation models. When the electric field over the polar cap extracts an electron beam, the particle number density is expected to be $\sim 10^4$–$10^6$ larger than the corotation density, a value which is appropriate when the angle between the angular velocity and the magnetic moment is acute (Arons 1983*b*, 1986). This regime may also be appropriate when the angle between the angular velocity and the magnetic moment is obtuse, if the pairs are created by "sparks" formed when the particle emissivity of the surface is completely inhibited, since in this case the local positron beams created by the discharges have density comparable to the corotation density (Ruderman and Sutherland 1975), as in the electron beam case, and the voltage drops at the surface are similar. On the other hand, if the surface can emit an ion beam with density comparable to the corotation density, the resulting positron beam whose gamma-ray emission gives rise to the final pair plasma has much lower density, while the voltage drop is the same as in the electron beam case (Arons 1983*b*). Since the pair density is proportional to the lepton beam density, with the proportionality constant being a function of the voltage drop on each field line (the same, in ion emitting and electron emitting polar caps), the final pair density in the outflow over a polar cap that can freely emit heavy ions is expected to be much lower than in the electron emission case, probably only $10^2$–$10^3$ times the corotation density. Intermediate cases when the ion emission is partially free (Cheng and Ruderman 1980; Jones 1979, 1982) should lead to intermediate results.

In all of these models, the energy density, $c$ times the momentum density, and parallel pressure of the resulting plasma are approximately equal to the energy density dissipated in the surface acceleration zone, diluted by the divergence of the field lines along which the plasma flows, or

$$U \approx c\Pi \approx P_{\parallel} \approx J_{\parallel}\,\Delta\Phi/c \approx [\epsilon B^2(R_*)/2\pi](\Omega_* R_*/c)^3(R_*/r)^3 . \tag{44}$$

Here $J_\parallel = B/P$, $\Omega_* = 2\pi/P$, the radial scaling assumes the field is dipolar, $\Delta\Phi$ is the voltage drop developed near the surface along $\boldsymbol{B}$ between the surface and the pair formation front where pair creation shorts out almost all of $E_\parallel$, and $\epsilon$ is the fraction of the cross-cap, corotation potential drop contained in $\Delta\Phi$. Typically, $\epsilon$ ranges from $\sim 10^{-4}$ in a strong field, rapidly rotating pulsar such as the Crab to about unity in an object near to cessation of pair creation, periods typically on the order of a few seconds (Barnard and Arons 1982, and references therein). Note that $4\pi U/B^2 \approx \epsilon(r/R_L)^3$, with $R_L$ the light cylinder radius, equal to $c/\Omega_*$. In the $O$-mode, the departure of $n^2$ from unity due to the polarization drifts, which contribute the terms proportional to $B^{-2}$, are of order $\epsilon$ compared to the order unity effects of the longitudinal response along $B$, which contribute the terms proportional to $\omega/\omega_p$. Therefore, we assume $B = \infty$ in the $O$-mode dispersion relation in all the plasma terms. The corrections due to vacuum polarization are also small compared to the longitudinal plasma polarizability, so we set $a = 1$. Then the $O$-mode dispersion relation is

$$(\omega^2 - c^2k_\parallel^2)\left(1 - \sum_s \frac{\omega_{ps}^2}{\omega^2} g_s\right) - c^2k_\perp^2 = 0 , \tag{45}$$

with

$$g_s = P\int_{-\infty}^{\infty} \frac{du_\parallel f_s(u_\parallel)}{\gamma^3(1 - n_\parallel \beta)^2} + i\pi\beta_\phi \gamma_\phi^3 S(\beta_\phi) f_s'(u_\phi) . \tag{46}$$

Here $\beta_\phi = \omega/ck = n_\parallel^{-1}$, $\gamma_\phi = (1 - \beta_\phi^2)^{-1/2}$, $u_\phi = \beta_\phi \gamma_\phi$, $S(\beta_\phi) = 1$ if $|\text{Re } \beta_\phi| < 1$ and $S(\beta_\phi) = 0$ if $|\text{Re } \beta_\phi| \geq 1$. Expression (46) was obtained by analytically continuing the integral in equation (32) over the whole plane of the complex index of refraction, and is uniformly valid on the complex $n$-plane except on a branch cut extending from the branch points $\beta_\phi = \pm 1$. We choose this cut to extend from $\beta_\phi = \pm 1$ to $\beta_\phi = -i\infty$ along the lines Re $\beta_\phi = \pm 1$. The principal value integral is the integral when $|\text{Re } \beta_\phi| > 1$; for such superluminous waves, the linear index of refraction is purely real. We are interested only in waves with weak damping or growth, for which Im $(n) \ll$ Re $(n)$; this motivates our choice of the branch cut. We neglect contributions from the branch cut itself; this contributes only to transient response to initial disturbances (Aaron and Currie 1966), which is not of importance here.

If one assumes $B = \infty$ in the $X$-mode dispersion relation $D_X = 0$, while at the same time vacuum polarizability is neglected, then $X$-mode propagation reduces to propagation in a perfect vacuum. At most altitudes of interest to wave propagation in radio pulsar magnetospheres, $\epsilon(r/R_L)^3 \gg b$, with $b$ given by equation (2). Then the effects of vacuum polarization are negligible, and the $X$-mode dispersion relation is

$$c^2k^2\left(1 - \frac{4\pi P_\parallel}{B^2}\cos^2\theta\right) + 2\omega ck\left(\frac{4\pi c\Pi}{B^2}\cos\theta\right) - \left(1 + \frac{4\pi U}{B^2}\right)\omega^2 = 0 , \tag{47}$$

with $\theta$ the angle between $\boldsymbol{k}$ and $\boldsymbol{B}$.

## III. PROPERTIES OF THE ORDINARY MODE WHEN B IS INFINITE

We have evaluated equation (46) for an electron-positron plasma with equal number densities of electrons and positrons and equal momentum distribution functions for two simple distributions: (1) a $\delta$-function in momentum, $f(u_\parallel) = \delta(u - u_0)$; and (2) for a "waterbag" distribution, $f(u_\parallel) =$ constant, $u_0 < u_\parallel < u_m$, with $f = 0$ outside this range. In addition, we have evaluated the dispersion relation approximately for arbitrary distribution functions. Since the distribution functions are identical, we have $\sum_s g_s \omega_{ps}^2 = g\omega_p^2$, where $\omega_p^2 = 8\pi e^2 N/m$. The quantity $N$ is the electron or positron density in the corotating frame, and $m$ is the electron rest mass.

### *a) Delta-Function Distribution*

When $f(u_\parallel) = \delta(u_\parallel - u_0)$, then $g = 1/[\gamma_0^3(1 - \beta_0 ck_\parallel/\omega)^2]$, and equation (46) becomes

$$(\omega^2 - c^2k_\parallel^2)\left[1 - \frac{\omega_p^2}{\gamma_0^3\omega^2(1 - \beta_0 ck_\parallel/\omega)^2}\right] - c^2k_\perp^2 = 0 . \tag{48}$$

For this distribution, there exists a frame in which the plasma is at rest, in which the density $N'$ is related to the laboratory density by $N = \gamma_0 N'$, so that $\omega_p = \gamma_0^{1/2}\omega_p'$. The $O$-mode dispersion relation in this comoving frame is obtained from equation (48) by setting $\beta_0 = 0$:

$$(\omega'^2 - c^2k_\parallel'^2)(1 - \omega_p'^2/\omega'^2) - c^2k_\perp'^2 = 0 . \tag{49}$$

Expressed in terms of $\theta'$, the angle with respect to the field, and the magnitude of $\boldsymbol{k}$ this is rewritten alternatively as

$$(ck'/\omega')^2 = [1 - (\omega_p'/\omega')^2]/[1 - (\omega_p' \cos\theta'/\omega')^2] ,$$

with solution

$$\omega'^2 = \tfrac{1}{2}\omega_p'^2\{1 + (ck'/\omega_p')^2 \pm [(1 + x^2)^2 - 4x^2\cos^2\theta']^{1/2}\} \tag{50}$$

Here $x = ck'/\omega_p'$. Equation (49) is plotted for several values of $k_\perp$ in Figure 1. From Figure 1 the two branches are evident; the fast (with comoving parallel index of refraction, $n_\parallel' \equiv ck_\parallel'/\omega' < 1$) and the Alfvén (with $n_\parallel' > 1$).

The polarization is found from equation (41) with $J_\parallel = 0$ and $a = 1$. Upon using equation (49) to express $(\omega'/\omega_p')^2$ in terms of

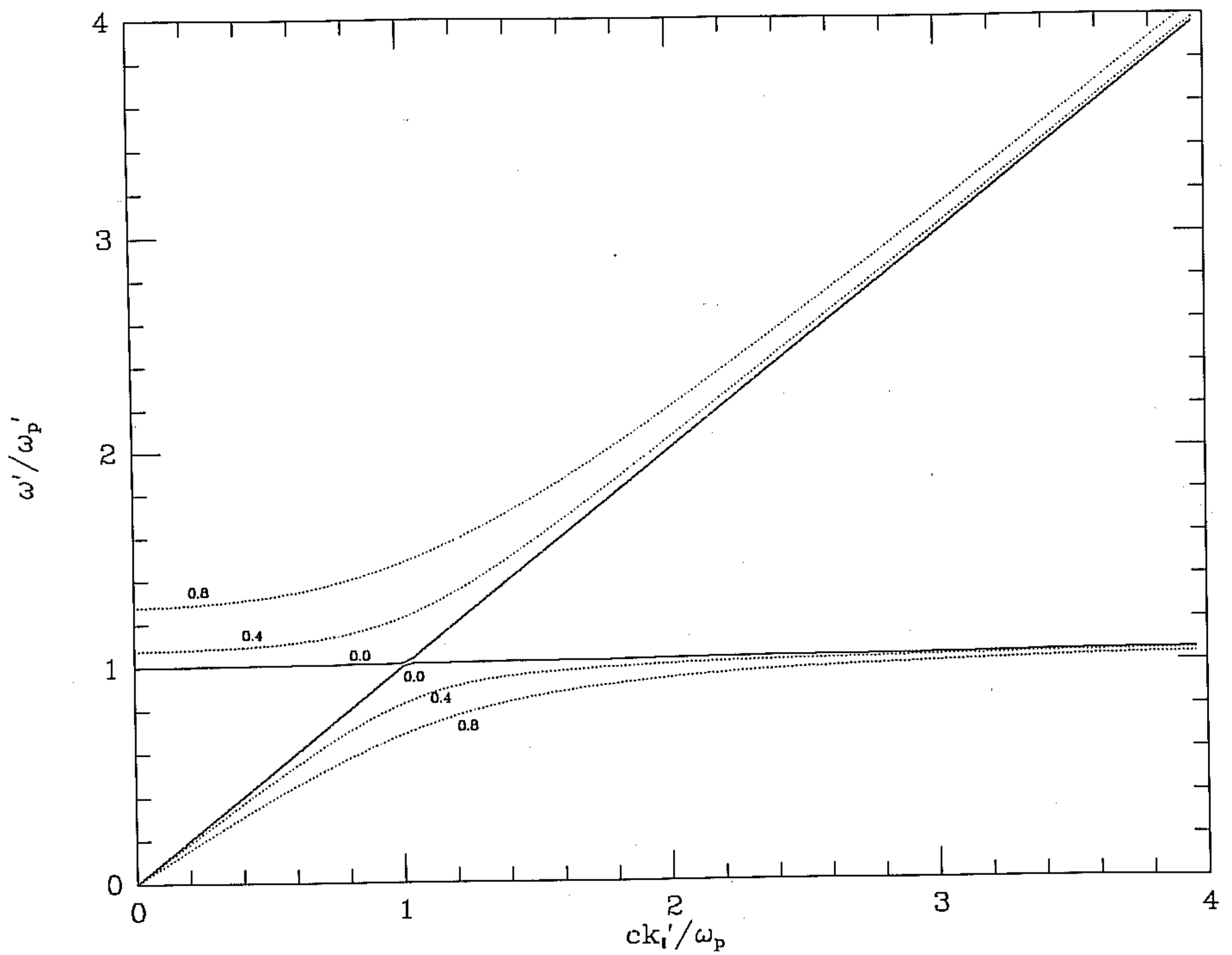


FIG. 1.—Dispersion relation for a cold electron-positron plasma in the rest frame of the plasma. Each curve is for a constant value of $ck_\perp'/\omega_p'$ labeled adjacent to the curve.

$x \equiv ck'/\omega_p'$ and $\theta'$, we find

$$\frac{\delta E_\parallel'}{\delta E_\perp'} = -\frac{2k_\perp' k_\parallel' c^2}{[\omega_p'^2 + k_\perp'^2 c^2 - k_\parallel'^2 c^2 \pm (\omega_p'^2 + k'^2 c^2)^2 - 4k_\parallel'^2 c^2 \omega_p'^2]^{1/2}} . \tag{51}$$

The slow (Alfvén) branch corresponds to choosing the minus sign, while the fast, superluminous branch is found by choosing the plus sign. In the limit $ck' \ll \omega_p'$,

$$\frac{\delta E_\parallel'}{\delta E_\perp'} \approx \begin{cases} -\left(\dfrac{ck'^2}{\omega_p'}\right) \sin\theta' \cos\theta' = -\dfrac{c^2 k_\parallel' k_\perp'}{(\omega_p')^2} & \text{(Alfvén branch)} \quad (52a) \\[2ex] \left(\dfrac{\omega_p'^2}{ck'}\right) \dfrac{1}{\sin\theta' \cos\theta'} = -\dfrac{(\omega_p')^2}{c^2 k_\parallel' k_\perp'} . & \text{(fast branch)} \quad (52b) \end{cases}$$

Equation (52a) shows that when the wave electric field appears to the plasma as an almost static field ($\omega_p' \gg \omega'$), the rapid mobility of the plasma along $\boldsymbol{B}$ almost completely shorts out $\delta \boldsymbol{E} \cdot \boldsymbol{B}$. The strong magnetic field inhibits similar shorting of the perpendicular currents driven by the wave, here entirely given by the displacement current across $\boldsymbol{B}$. The mode is simply the Alfvén wave of magneto hydrodynamics, in the regime when displacement current greatly exceeds conduction current. Because $\delta E_\parallel' \approx 0$, the Poynting flux is almost along $\boldsymbol{B}$, not $\boldsymbol{k}'$. This is the same as in the usual Alfvén wave derived for $4\pi B^2 \ll U$; Alfvén wave ducting of energy along $\boldsymbol{B}$ depends on $\delta E_\parallel' \approx 0$, not on the "twanging" of field lines. Equation (52b) shows that the wave on the fast branch has become an oscillation at the plasma frequency polarized along $B$ in the long wavelength limit $k' \ll \omega_p'/c$.

In the low density, short wavelength regime $k' \gg \omega_p'/c$,

$$\frac{\delta E_\parallel'}{\delta E_\perp'} \approx \begin{cases} \dfrac{k_\parallel'}{k_\perp'}\left[1 + O\left(\dfrac{\omega_p'}{ck'}\right)^2\right] & \text{(Alfvén branch)} \quad (53a) \\ -\dfrac{k_\perp'}{k_\parallel'}\left[1 + O\left(\dfrac{\omega_p'}{ck'}\right)^2\right] & \text{(fast branch)} \quad (53b) \end{cases}$$

Equation (53a) shows that the short wavelength limit of the Alfvén wave is a plasma oscillation polarized along $k'$ ($k' \times \delta E' \approx 0$), while the fast branch of the $O$-mode has become a vacuum electromagnetic wave which can escape to infinity ($k' \cdot \delta E \approx 0$). These identifications are all supported by the solutions (50).

In Figure 2, the dispersion relation for waves observed in the laboratory frame is plotted (i.e., eq. [5]). Since Figure 1 is related to Figure 2 by a Lorentz transformation of $k'$ and $\omega'$, leaving $\omega'^2 - c^2k_\parallel'^2$ invariant, the branches are still divided into those with phase velocities above and below the speed of light. An important difference, however, is that if $k_\perp$ is sufficiently small, plasma effects which are important only near the plasma frequency $\omega_p'$ in the comoving frame extend from $\omega = \omega_p'/\gamma_0 = \omega_p/\gamma_0^{3/2}$ to $\omega = (1 + \beta_0)\gamma_0\,\omega_p' = (1 + \beta_0)\gamma_0^{1/2}\omega_p$ in the laboratory frame. For example, this Doppler smearing of the plasma resonance covers four decades in $\omega$ for $\gamma_0 = 100$.

### b) *Waterbag Distribution*

Since the plasma streaming along pulsar open field lines is expected to have a broad, relativistic distribution, the cold-plasma approximation will be inappropriate in certain regimes. To model the behavior of a hot plasma we use a flat or "waterbag"

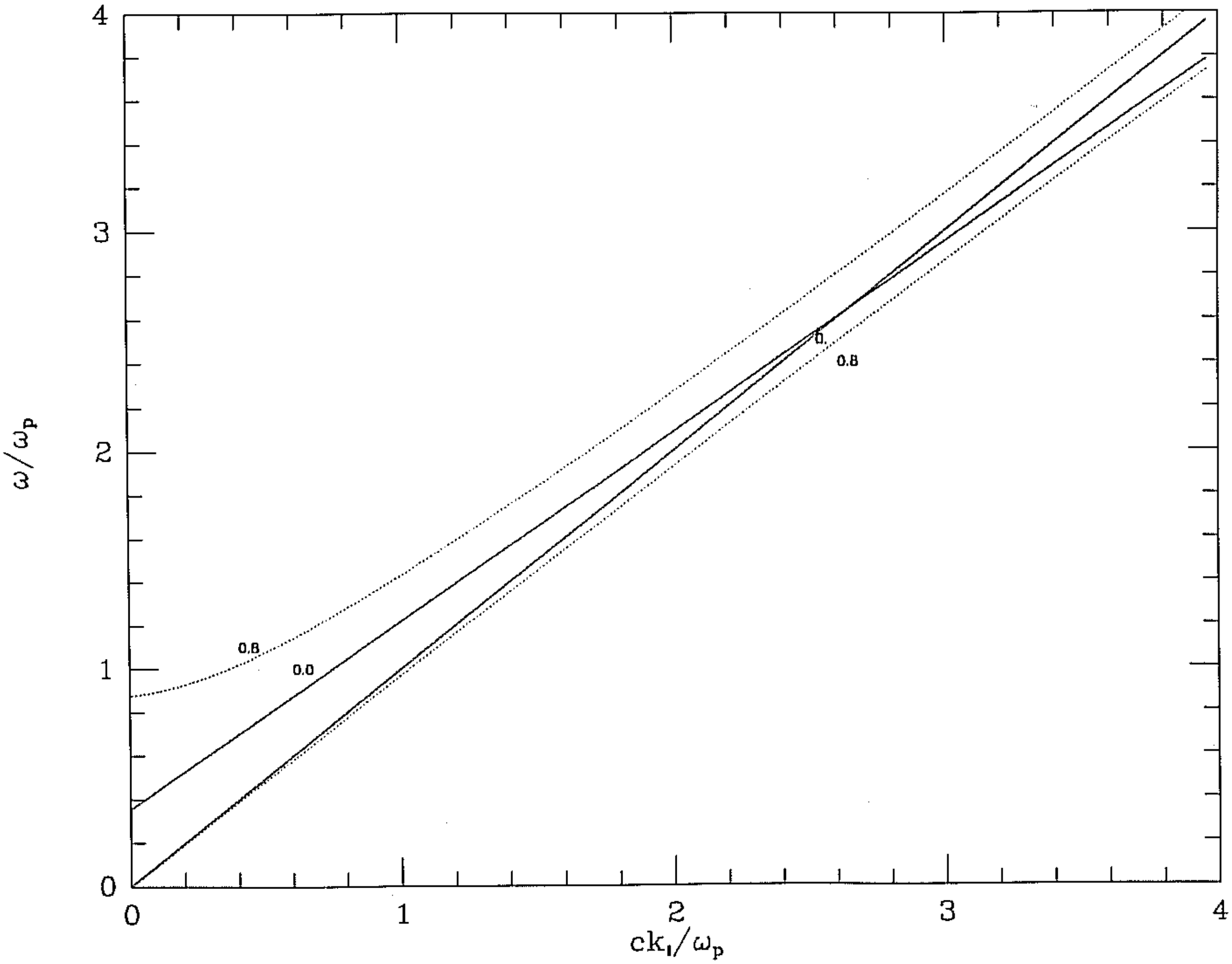


FIG. 2.—Dispersion relation for a cold electron-positron plasma with relativistic flow velocity ($\gamma = 2$), with two values of $ck_\perp/\omega_p$ shown.

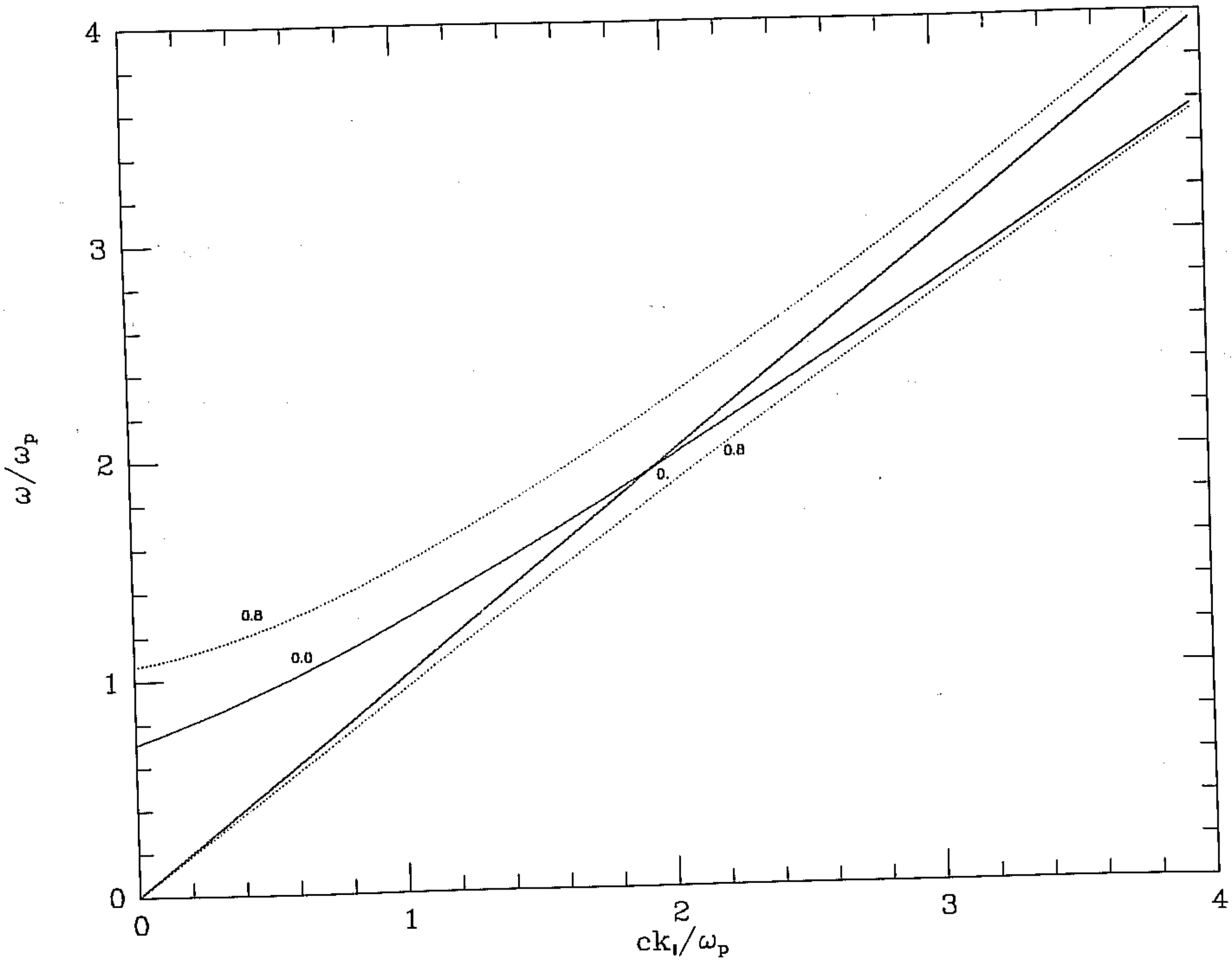


FIG. 3.—Dispersion relation for the waterbag distribution function. Here $\gamma_m = 2$ and $\gamma_0 = 1$. Two values of $ck_\perp/\omega_p$ (0.0 and 0.8) are shown.

distribution such that

$$f(u_\parallel) = \begin{cases} 1/(u_m - u_0) & u_0 < u_\parallel < u_m \\ 0 & \text{otherwise} \end{cases} . \tag{54}$$

Using equation (54) in equation (46) yields:

$$g = \frac{1}{\gamma_m \beta_m - \gamma\beta}\left(\frac{\beta_m}{1 - \beta_m n_\parallel} - \frac{\beta_0}{1 - \beta_0 n_\parallel}\right) . \tag{55}$$

The solution to equation (46) using equation (55) is plotted in Figure 3, using, as an example, $\gamma_m = 2$ and $\gamma_0 = 1$; these low values of $\gamma_m$ and $\gamma_0$ are chosen for graphical clarity. The main qualitative difference between the dispersion relations for the two distributions is that for the waterbag distribution no wave modes exist with phase velocities between $\beta_0$ and $\beta_m$, whereas for the cold distribution (which, in fact, is the limit $\gamma_m - \gamma_0 \to 0$) all phase velocities are present.

### c) *General Features of the Dispersion Relation*

For a general distribution, the superluminous branch of the *O*-mode has a low-frequency cutoff (when the total index of refraction $n$ vanishes) at

$$\omega_{\text{cutoff}} = \langle 1/\gamma^3 \rangle^{1/2} \omega_p , \tag{56}$$

where the angle brackets denote average over the momentum distribution. When $k_\perp = 0$, the two branches of the dispersion relation cross at

$$\omega_{\text{cross}} = \langle (1 + \beta)^2 \gamma \rangle^{1/2} \omega_p \approx 2 \langle \gamma \rangle^{1/2} \omega_p . \tag{57}$$

As an example, for a power-law distribution, in which $f(\gamma) \propto \gamma^s$ between $\gamma_0$ and $\gamma_m$, and in which $\gamma_m \gg \gamma_0 \gg 1$, the cutoff frequency is given by

$$\omega_{\text{cutoff}}^2 = \omega_p^2\left(\frac{s+1}{s-2}\right) \times \begin{cases} 1/\gamma_0^3 & s < -1 \\ 1/(\gamma_0^{2-s}\gamma_m^{s+1}) & -1 < s < 2\,, \\ 1/\gamma_m^3 & 2 < s \end{cases} \tag{58}$$

and $\omega_{\text{cross}}$ for the same distribution is

$$\omega_{\text{cross}}^2 = \omega_p^2 \frac{4(s+1)}{(s+2)} \times \begin{cases} \gamma_0 & s < -2 \\ \gamma_m^{s+2}\gamma_0^{-s-1} & -2 < s < -1\,. \\ \gamma_m & s > -1 \end{cases} \tag{59}$$

Thus the range of frequencies over which plasma effects are important for the fast mode remains large in a hot plasma:

$$\frac{\omega_{\text{cross}}}{\omega_{\text{cutoff}}} = \frac{2\langle\gamma\rangle^{1/2}}{\langle 1/\gamma^3\rangle^{1/2}} = 2\left|\frac{s-2}{s+2}\right|^{1/2} \begin{cases} \gamma_0^2 & s < -2 \\ \gamma_0^{1-(s/2)}\gamma_m^{1+(s/2)} & -2 < s < 2\,. \\ \gamma_m^2 & s > 2 \end{cases} \tag{60}$$

The behavior of the fast mode is modified by finite momentum dispersion only when the distribution function is relatively flat $(-2 < s < 2)$. If $s > 2$, the dispersion relation behaves like a $\delta$-function at $\gamma_{\max}$, and if $s < -2$, like a $\delta$-function at $\gamma_{\min}$.

We may evaluate equation (46) approximately for arbitrary distribution functions and solve for $n_\parallel$, by using two asymptotic limits:

$$g = \int \frac{f du_\parallel}{\gamma^3(1-\beta n_\parallel)^2} \approx \begin{cases} \left\langle \dfrac{1}{\gamma^3} \right\rangle (1-n_\parallel)^{-2} & \text{Regime A: } |1-n_\parallel| \gg \dfrac{1}{2\gamma_t^2} \quad (61a) \\ 4\langle\gamma\rangle & \text{Regime B: } |1-n_\parallel| \ll \dfrac{1}{2\gamma_t} \quad (61b) \end{cases}$$

Here

$$\gamma_t \equiv \langle 1/\gamma^3\rangle^{-1/4}\langle\gamma\rangle^{1/4}\,. \tag{62}$$

In regime A, assuming $(1+n_\parallel) \approx 2$, equation (45) has the solutions

$$1 - n_\parallel = (\tfrac{1}{2})[n_\perp^2/2 \pm (n_\perp^4/4 + 4\alpha)^{1/2}]\,. \tag{63}$$

Here

$$\alpha = \omega_{\text{cutoff}}^2/\omega^2 \equiv \langle 1/\gamma^3\rangle\omega_p^3/\omega^2\,, \tag{64}$$

and note that $\omega_{\text{cross}}^2/\omega^2 = 4\gamma_t^4\alpha$.

In regime B $|1-n_\parallel| \ll 1/(2\gamma_t^2)$, and equation (3) yields

$$1 - n_\parallel \approx \frac{n_\perp^2}{2(1 - 4\langle\gamma\rangle\omega_p^2/\omega^2)}\,. \tag{65}$$

The transition between regime A and regime B occurs when equation (63) is set equal to equation (65), which requires $n_\perp$ to satisfy

$$n_\perp = (1/\gamma_t)|1 - 4\gamma_t^4\alpha|^{1/4}\,. \tag{66}$$

Since equation (45) (together with eq. [61a]) is a quartic equation in $n_\parallel$, for each $\alpha$ there are four values of $n_\parallel$ which satisfy equation (46), two each on the fast and Alfvén branches. However, one solution has $n_\parallel \approx -1 + n_\perp^2/2$ (a backward-propagating fast mode wave in both laboratory and comoving frames), and one solution corresponds to a plasma wave with phase velocity comparable to the range in comoving particle velocities expected in a realistic distribution function, and so will have a large imaginary part to the frequency (see § IV). We restrict our attention to the other two solutions which are outward propagating and have small imaginary $\omega$.

Expanding equations (63), (65), and (66) yields the following asymptotic formula for $1 - n_\parallel$:

Fast mode:

$$1 - n_\parallel \approx \begin{cases} n_\perp^2/2 + 2\alpha/n_\perp^2 & n_\perp/2 \gg \alpha^{1/2} \quad \text{and} \quad 1/2\gamma_t^2 & (67a) \\ \alpha^{1/2} + n_\perp^2/4 & \alpha^{1/2} \gg n_\perp^2/2 \quad \text{and} \quad 1/2\gamma_t^2\,. & (67b) \\ (n_\perp^2/2)(1 + 4\gamma_t^4\alpha) & 1/2\gamma_t^2 \gg \alpha^{1/2} \quad \text{and} \quad n_\perp^2/2 & (67c) \end{cases}$$

Alfvén mode:

$$1 - n_\parallel \approx \begin{cases} -n_\perp^2/8\gamma_t^4\alpha & \alpha^{1/2} \gg 1/2\gamma_t^2 \quad \text{and} \quad \alpha^{1/2} \gg n_\perp/2\gamma_t \\ \text{see text} & \text{otherwise} \end{cases} . \tag{68a, 68b}$$

If the conditions on equation (68) are not met, then $1 - n_\parallel \approx 1/2\gamma_t^2$, and again Im $\omega$ becomes large.

For a physical understanding of refractive and other effects, it is useful to have an expression for the phase velocity (in units of the speed of light) which from eqation (46) is

$$\beta_{\rm ph} \equiv 1/n[1 - (1 - n_\parallel^2)g\omega_p^2/\omega^2]^{1/2} . \tag{69}$$

Inspection of equation (69) shows that $n$ greater than (less than) unity implies that $\beta_{\rm ph}$ is less than (greater than) unity. Therefore, in the above asymptotic regimes we have the following:

Fast mode:

$$\beta_{\rm ph} = \begin{cases} 1 + 2\alpha/n_\perp^2 - \alpha/2 & n_\perp^2/2 \gg 1/2\gamma_t^2 \quad \text{and} \quad \alpha^{1/2} & \text{(70a)} \\ 1 + \alpha^{1/2} + \alpha - n_\perp^2/2 & \alpha^{1/2} \gg 1/2\gamma_t^2 \quad \text{and} \quad n_\perp^2/2 \, . & \text{(70b)} \\ 1 + 2\gamma_t^4\alpha n_\perp^2 & 1/2\gamma_t^2 \gg n_\perp^2/2 \quad \text{and} \quad \alpha^{1/2} & \text{(70)c)} \end{cases}$$

Alfvén mode:

$$\beta_{\rm ph} = \begin{cases} 1 - \dfrac{1}{2} n_\perp^2 + \dfrac{3}{256\gamma_t^4\alpha} n_\perp^4 & \alpha^{1/2} \gg \dfrac{1}{2\gamma_t^2} \quad \text{and} \quad \alpha^{1/2} \gg \dfrac{n}{2\gamma_t} . & \text{(71)} \\ \text{see text} & \text{otherwise} & \text{(72)} \end{cases}$$

Thus, on the fast branch when $n_\perp$ is large (eq. [70a]) or when $n_\perp$ is small and the waves are plasma-like (eq. [70b]), increasing $n_\perp$ increases displacement current relative to plasma current, thus driving the phase velocity closer to that of a light wave in free space (i.e., $c$). However, when $n_\perp$ is near zero and the wave is already supported by displacement current (eq. [70]), increasing $n_\perp$ increases the electric field parallel to $b$, which increases the plasma current, making the phase velocity more superluminous. In Figure 4 we plot $\beta_{\rm ph} - 1$ as a function of $\omega_p^2/\omega^2$ for a cold distribution with $\gamma_0 = 100$ for several values of $n_\perp$.

On the Alfvén branch, the same arguments apply, although essentially in reverse. When $n_\perp$ is small and the wave is purely electromagnetic (see eq. [71]), increasing $n_\perp$ increases plasma current, which decreases the phase velocity. Again, when the conditions on equation (70a) are not met, the parallel phase velocity is comparable to the particle velocity, so that Landau damping or growth occurs, and the implicit assumption that the wave frequency be much greater than the damping or growth rate is violated. In this regime the real and imaginary parts of $\omega$ depend sensitively on the exact form of the distribution function.

## IV. DAMPING OF ALFVÉN WAVES IN AN OUTFLOWING PLASMA

In the previous section, we found solutions for the index of refraction with damping completely neglected. In the $B = \infty$ approximation, linear damping of the $X$-mode due to wave particle resonance is absent because no particles exist with speed equal to $c$. Likewise, there is no damping of waves on the superluminous branch of the $O$-mode. For all waves in radio pulsar plasmas, collisional damping is negligible. However, the Alfvén wave branch of the $O$-mode can interact resonantly with the particles. In an electron-positron plasma with identical distribution functions for each species, this can lead to damping at rates which constrain the presence of such waves in the magnetosphere. In this section, we consider this effect, using a very simplified model of the pair distribution functions.

We assume the pair distribution functions are given by

$$f_\pm(u_\parallel) = \begin{cases} u_m^{-1} \exp\,[-(u_\parallel - u_0)/u_m] & u_\parallel \geq u_0 \gg 1 \\ 0 & u_\parallel < u_0 \end{cases} . \tag{73}$$

This represents a relativistically outflowing plasma with the expected broad momentum dispersion and the relativistic low-energy cutoff set by the finite opacity for pair creation above the poles. We expect, and will show, that the Alfvén waves which propagate outward along the open field lines are weakly damped if and only if their phase momentum $u_\phi = \beta_\phi \gamma_\phi$ exceeds the exponential cutoff momentum $u_m$. Then from equation (68a) evaluated for this distribution,

$$n_\parallel \approx 1 + \frac{n_\perp^2}{8u_m}\frac{\omega^2}{\omega_p^2} \tag{74}$$

gives the index of refraction, neglecting damping. This dispersion relation is correct if $4u_m\omega_p^2 \gg \omega^2$ and $\omega_p^2/u_0\,\omega^2 \gg n_\perp^2/2$. Notice that if $\omega_p$ becomes very large, equation (74) predicts the wave propagates with speed approaching the speed of light along the field lines, since at very high density, the component of $\delta E$ along $B$ is almost completely shorted out.

One might expect that at high density, the finite cross field drifts might make a more important contribution to the dispersion, as in ordinary hydromagnetic waves. However, if one assumes very large plasma frequency in equation (44), along with propagation along $B$ with $n_\parallel - 1 \ll u_m^{-2}$ and with the distribution function given by equation (73), then

$$\frac{(n_\parallel - 1)_{\rm HM}}{(n_\parallel - 1)_{B=\infty}} = \frac{\omega_p^4}{4\omega^2\omega_c^2 u_0^2} = \frac{\pi N mc^2}{B^2 u_0^2}\frac{\omega_p^2}{\omega^2} , \tag{75}$$

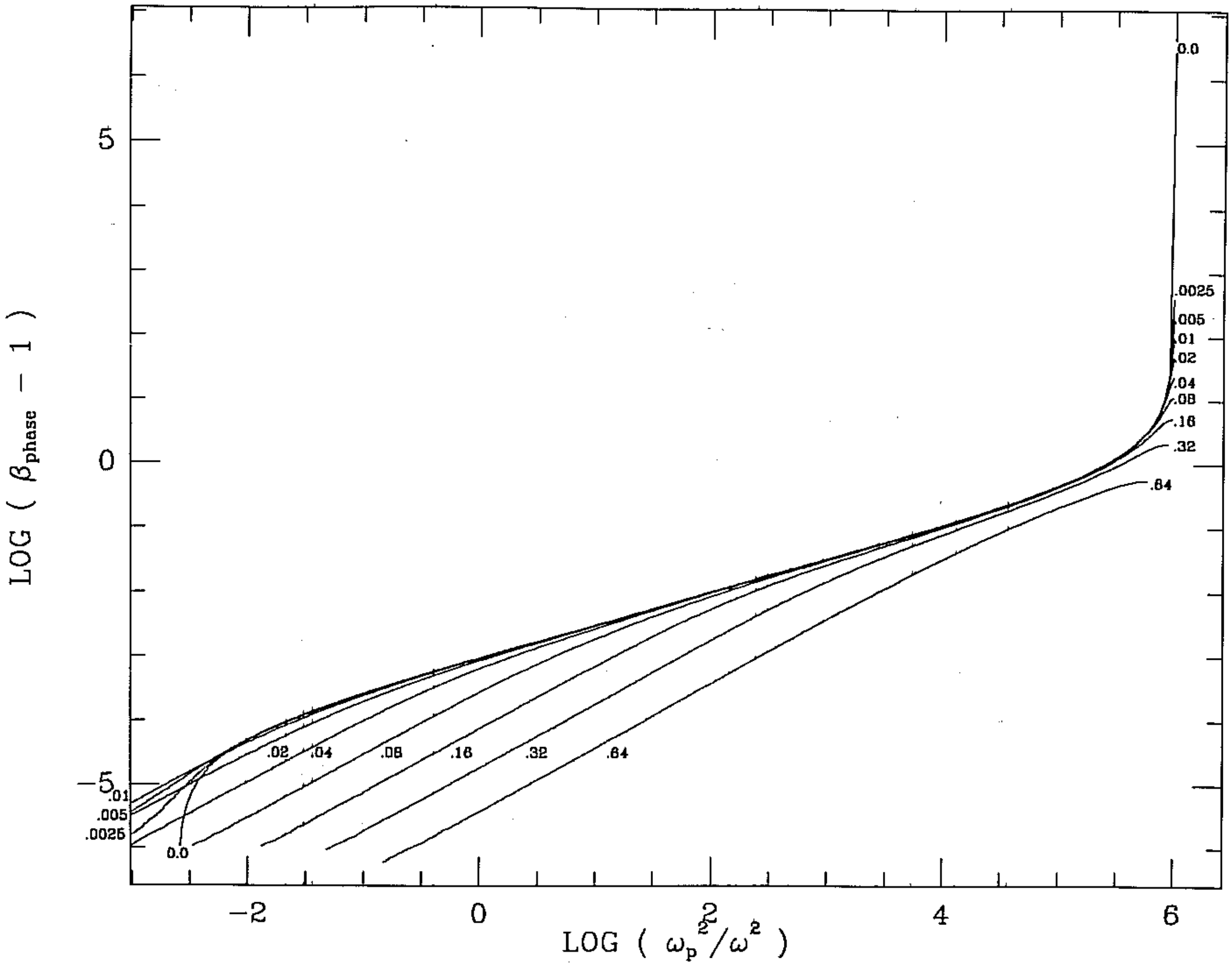


FIG. 4.—Departure of the phase velocity (in units of $c$) from unity for the fast mode of a cold flowing $e^{\pm}$ plasma ($\gamma_0 = 100$). Ten different values of $n_\perp$ are labeled. The asymptotic forms represented in eqs. (70$a$)–(70$c$) are found in the parallel curves in the lower left, the solid curve forming an upper envelope, and the down turning curves in the extreme lower left, respectively.

where $(n_\parallel - 1)_{\rm HM}$ is the index of refraction for almost parallel propagation with $\delta E_\parallel$ neglected, and $(n_\parallel - 1)_{B=\infty}$ is the index of refraction from equation (74). This ratio is independent of position for relativistic outflow along $B$ with no acceleration of the particles. Even for densities as high as $10^6$ times the corotation density, the numerical value of equation (75) is $10^{-5}/u_0^2$. Therefore, in the main body of the pair distribution, the $B = \infty$ approximation is excellent.

We now write the basic $O$-mode dispersion relation (45) in the form

$$D(\omega, k, \theta) = \omega^2 - c^2k^2 - (\omega^2 - c^2k_\parallel^2)\frac{\omega_p^2}{\omega^2}\, g(n_\parallel) = 0 \,, \tag{76}$$

with $g$ given by equation (46). When $n_\parallel$ is given by equation (73), we find $g \approx 4u_m + i\pi\beta_\phi\gamma_\phi^3 f'$. We now assume $k = k_r + ik_i$, with $k_i \ll k_r \approx k$ and write $D \approx D_r(\omega, k_r, \theta) + iD_i(\omega, k_r, \theta) + ik_i(\partial D_r/\partial k)_{k_i=0} = 0$. Since $k_r(\omega)$ is determined by $D_r(\omega, k_r, \theta) = 0$, this yields $k_i = -D_i/(\partial D_r/\partial k)$. We now evaluate this general result with the dispersion relation (73), to find

$$k_i = \frac{\pi}{4}\, k\, \frac{\omega_p}{u_m^{5/2}\omega\theta} \exp\left(-\frac{2\omega_p}{u_m^{1/2}\omega\theta}\right) \tag{77}$$

where we have self-consistently assumed $n \approx 1$ and $\theta \ll 1$.

We now apply this result to a simplified picture of wave propagation. Suppose the radiation is emitted with $\boldsymbol{k}$ along $\boldsymbol{B}$ in a low-altitude region of the magnetosphere, where $\omega \ll \omega_p$. An example of such a region might be the plasma zone just above the "gap" or "starvation zone" which forms in a variety of models for pair creation (see Arons 1983$b$ for a summary of these). Tsytovitch and Kaplan (1972) have outlined at least one emission mechanism for the production of field-aligned Alfvén waves, which may be applicable to the relativistic plasmas expected in the pair creation models. Above this wave generation zone, the relaxation of the bump-on-tail character of the plasma which causes the emission requires the waves to propagate through stable plasma, before being converted into waves on the superluminous branch of the $O$-mode. This conversion must occur by nonlinear mode coupling or by linear gradient coupling, topics outside of our present study. The simplest model for the plasma structure is relativistic plasma outflow along a dipole magnetic field, with no gradients in the distribution functions across $B$ and with density declining in proportion to $r^{-3}$ but no other variation of the distribution functions with $r$. Then $\omega_p/\omega$ decreases with altitude, while the phase 4-velocity

$$u_\phi = \beta_\phi \gamma_\phi = \frac{2u_m^{1/2}\omega_p}{n_\perp \omega} \tag{78}$$

also decreases, and $k_\parallel/k$ increases with radius.

Consider emission at radius $r_e$ along a field line whose footprint intersects the crust at magnetic colatitude $\Theta_*$. In the accompanying paper, we show that if an Alfvén wave is emitted with $k$ exactly along $B$, the angle between $k$ and $B$ at each point along a ray is

$$\theta = \frac{3}{8}\Theta_e\left(\frac{r}{r_e}\right)^{1/2}\left(1 - \frac{r_e}{r}\right)^2 , \tag{79}$$

where $\Theta_e = \Theta_*(r_e/R_*)^{1/2}$ is the magnetic colatitude of the emission point, when $1 \gg \Theta_e > \Theta_*$. Our dispersion relation (73) is correct if $u_\phi/u_m \gg 1$. From equations (79) and (78), this propagation, with the phase momentum on the tail of the pair distribution, occurs for all radii $r < r_m$, where

$$\frac{r_m}{R_*} \approx 120\left(\frac{100}{u_m}\right)^{1/4}\left[\frac{n_{\rm pair}(R_*)}{10^{16}\ {\rm cm}^{-3}}\right]^{1/4}\left(\frac{\lambda}{1\ {\rm m}}\right)^{1/2}\left(\frac{0.1}{\Theta_e}\right)^{1/2}\left(\frac{r_e}{R_*}\right)^{1/4} . \tag{80}$$

Alfvén waves emitted anywhere between the surface and $\sim 1000$ km satisfy this condition, if the emission occurs in the densest parts of the pair plasma.

Landau absorption is more important in constraining the range of radii where waves can propagate on the low-frequency branch. The spatial damping rate of the energy density is $2k_i$. The optical depth for waves emitted at $r_e$ to reach $r$ is

$$\tau(r, r_e) = \int_{r_e}^{r} 2k_i(r', r_e)dr' \approx \frac{\pi}{6}\frac{kr}{u_m^2}\exp\left[-\frac{8}{3}\frac{\omega_p(r)}{u_m^{1/2}\omega\Theta_e}\right] , \tag{81}$$

assuming $r - r_e > r_e$, as must be the case if the radiation is to escape from low altitude to infinity. This optical depth is strongly frequency dependent, while pulsar spectra show no signs of exponential cutoffs in the radio range. Therefore, the optical depth between the emission zone and the region of mode conversion to the escaping branch of the $O$-mode must be less than unity. This restricts the region of Alfvén wave transport to be at radii less than $r_{\rm abs}$, with $r_{\rm abs} = r_m/(\ln \Lambda)^{1/2}$ and

$$\ln \Lambda = 3.2 + \ln (r/100\ {\rm km}) - \ln (\lambda/1\ {\rm m}) - \ln (u_m/100)^2 + \ln (r/r_e)^2 . \tag{82}$$

Thus if the radio emission process is at very low altitude on polar field lines and the radiation must propagate to infinity through a relativistically streaming plasma which is stratified only in the radial direction, the lack of strong Landau absorption in the observed radio spectra implies the efficient conversion of this radiation into the superluminous $O$-mode at radii less than 1000 km, for canonical parameters of polar flow models for radio pulsars. This conclusion is not changed if one assumes a power-law distribution for the high-energy tails of the particle distributions. This changes the exponential dependence of the optical depth on $\omega$ into a power-law dependence, but the absorption still implies an exponential cutoff of the radiation spectrum above a critical frequency.

## V. PROPAGATION CHARACTERISTICS OF THE EXTRAORDINARY MODE

When the current and charge densities have their "normal" values, $J_\parallel/B \approx P^{-1}$ and $c\eta/B \approx P^{-1}$, the $O$- and $X$-modes decouple, and the $X$-mode dispersion relation is $D_X = 0$, with $D_X$ given by equation (33). The wave is linearly polarized, with $\delta E$ perpendicular to the plane of $k$ and $B$, and $\delta B$ in the plane of $k$ and $B$. For plasma at rest with vacuum polarization neglected, the explicit solution of the dispersion relation is

$$\omega^2 = c^2k^2\left(1 - \frac{4\pi P_\parallel}{B^2}\cos^2\theta\right)\left(1 + \frac{4\pi U}{B^2}\right)^{-1} . \tag{83}$$

This dispersion relation and the associated polarization identify the $X$-mode as the magnetosonic wave of magnetohydrodynamics, with relativistic energy density and displacement current included (1 is added to $4\pi U/B^2$). Because the plasma is assumed to have only parallel momentum dispersion, the $X$-mode can be firehose unstable, if $P_\parallel$ exceeds the magnetic tension $B^2/4\pi$. If the plasma density approaches zero while the magnetic field remains strong ($\omega_{cs} \gg \omega$) for all species, the $X$-mode becomes a light wave, with phase and group speed approaching $c$ from below. If $4\pi U/B^2 \gg 1$, the wave propagates as the conventional magnetosonic mode, with phase and group velocity much less than $c$.

The $X$-mode dispersion relation can be solved in general. Define $a = c\Pi/U$ and $b = P_\parallel/U$ and let $\delta = 4\pi U/B^2$ and $\mu = \cos\theta$. Then

$$n = \{-a\mu\delta \pm [1 + (1 - b\mu^2)\delta + (a^2 - b)\mu^2\delta^2]^{1/2}\}/(1 - b\mu^2\delta) , \tag{84}$$

where $\theta < \pi/2$ and $n > 0$ corresponds to waves travelling outward from the star. For $\theta > \pi/2$, the outbound wave corresponds to

$n < 0$. We are interested in very strongly magnetized plasmas, with $\delta \ll 1$. Then

$$n = \pm[1 + \tfrac{1}{4}(1 \pm 2a\mu + b\mu^2)\delta] \tag{85}$$

through first order in $\delta$. If the plasma is cold with streaming velocity $v_\parallel = +c\beta_0$, then $a = \beta_0$ and $b = \beta_0^2$, and

$$n = \pm[1 + \tfrac{1}{2}\delta(1 \mp \beta_\parallel)^2] , \tag{86}$$

with $\beta_\parallel = \beta_0 \mu$. When the plasma is cold, the results (83)–(86) can be equally well derived by first Lorentz transforming to the rest frame of the plasma where $(\omega')^2 = c^2(k')^2/(1 + \delta')$, then transforming back to the streaming frame. When the plasma is hot with the distribution function given by equation (73), the $X$-mode index of refraction is still given by equation (86), with

$$\beta_0 = 1 - \frac{1}{2u_m^2}\left[\ln\left(\frac{u_m}{u_0}\right) - 0.577\right] . \tag{87}$$

In a magnetized plasma with transverse velocity dispersion and nonzero magnetic moments $\langle M \rangle$, the $X$-mode can be damped (Barnes 1966). The mechanism is the Landau damping of longitudinal components of the wave electric field, which appear because of $\langle M \rangle \cdot \nabla \delta B$ forces on the particles. In an electron-ion plasma, these act to separate electrons from ions, creating an electrostatic component of the wave electric field polarized along $B$. Barnes and Scargle (1973) showed that the same effect persists in an isotropic, relativistic plasma when the electron and ion distribution functions differ. In our model of a pulsar's plasma, such damping is absent, primarily because the plasma has no momentum dispersion transverse to $B$; this appears in the 2–3 and 3–2 components of the mobility tensor, which are exactly zero when $k_\perp$ is zero since the magnetic moments of all the particles are zero. In addition, if the distribution functions of the ultrarelativistic species are identical, then the Landau damping of the $X$-mode is zero even if the magnetic moments are finite. These special symmetries can be broken by various processes which can excite (small) pitch angle dispersion in the plasma and differentially accelerate the species, but these topics are beyond the scope of our work here.

## VI. CONCLUSION

### *a) Remarks on Propagation Characteristics and Emission Mechanisms*

The above constraints are meant to be illustrative examples, since we have omitted a variety of important effects which need to be included in a complete propagation model. Transverse stratification and relative streaming between the plasma components are of special importance, since these can lead to rapid refraction of the radiation into the boundary layers and continued growth of the modes, rather than damping, respectively. Once in the boundary layers, the steep gradients and large current and charge densities can lead to strong mode coupling and escape of radiation to infinity, rather than the damping implied by equation (81). The optical depth (eq. [81]) does show that it is not sufficient to simply propose an instability mechanism for the emission of high brightness temperature radiation; one must also specify the means of escape of this radiation to infinity. Most of the attractive pulsar models suggest the generation of coherent photons occurs in a plasma and magnetic field configuration with both the crossover frequency (eq. [56]) and the cyclotron frequency large compared to the wave frequency. Direct emission processes below the cyclotron frequency (e.g., Asseo, Pellat, and Sol 1983) couple only to subluminous radiation. Our results for Landau absorption show that if the radio emission occurs because of a mechanism of this sort, escape of this radiation to infinity requires mode conversion into superluminous waves which must occur at relatively low altitude, in order to avoid noticeable absorption effects in the spectra.

Models have been proposed in which low-altitude emission occurs along polar field lines in a relativistically outflowing electron-positron plasma with much lower density, such that the plasma frequency (more precisely, the crossover frequency) falls within the observed spectral domain (Ruderman and Sutherland 1975; Benford and Buschauer 1977; Cheng and Ruderman 1980; Stinebring *et al.* 1984*a*, *b*). In these, radio emission occurs because of a two-step process. The plasma is presumed to be electrostatically two-stream unstable, because of relative motion between the components. From our results in § III, this requires the special assumption $k_\perp/k \ll (\omega_p^2/\gamma^3\omega^2)^{1/4}$; if this inequality is violated, the instability is intrinsically electromagnetic, and the emission process is direct. The broad momentum dispersion in the pair plasma prevents growth of the electrostatic modes due to the relative streaming between the electrons and positrons proposed by Cheng and Ruderman (1977), while electrostatic instability driven by the high-energy beam accelerated in the surface starvation zone is too weak, if the beam is composed of TeV electrons or positrons (Benford and Buschauer 1977). If the surface can emit baryonic ions, the much lower longitudinal mass allows possible excitation of electrostatic modes (Buschauer and Benford 1977), subject to the very restrictive constraint on $k_\perp/k$.

Electrostatic beam plasma modes cannot escape from the magnetosphere, however. In all of these models, the authors hypothesize that the electrostatic instability operates solely to create charge density bunching in the plasma. These bunches radiate electromagnetic waves by the vacuum curvature process, enhanced by the collective organization of many charges within one vacuum wavelength. In essence, the collective emission process is the coupling of electrostatic plasma waves to vacuum curvature modes.

Because the emission must occur in a plasma, with the collective enhancement of the emission occuring at the proper plasma frequency, the Razin effect reduces the vacuum curvature emissivity of an electrostatically generated bunch. The results of Asseo, Pellat, and Sol (1983) show this to be the case for curvature emission into the $O$-mode; only bunching amplitudes in excess of unity lead to sufficient emissivity in bunched coherent curvature emission, if the mechanism were to generate only $O$-mode photons. Here, we give some preliminary considerations of possible Razin suppression of the $X$-mode emission.

If the emission process is to proceed as if in vacuum, the time retardation factor $1 - n\beta_0 \cos\theta$ must be well approximated by setting the index of refraction $n$ equal to unity, where $\theta$ is the angle between the $k$ vector of the radiation and $\boldsymbol{\beta}_0 = \beta_0 \boldsymbol{B}/B$, and $c\beta_0$ is the velocity of a group of emitting particles along $B$. From our approximate dispersion relation (86),

$$1 - n\beta_0 \cos\theta = \frac{1}{2\gamma_0^2}(1 + \gamma_0^2\theta^2) - \frac{\delta}{8\gamma^4}(1 + \gamma^2\theta^2)^2 . \tag{88}$$

The standard theory assumes $\delta = 0$. Suppose, first, that the emission is narrow band near the proper plasma frequency and occurs with maximum efficiency at each position, so that the vacuum critical frequency for curvature emission $\omega_{\rm crit} = 3c\gamma_0^3/\rho$ is near the crossover frequency (eq. [56]). Here $\rho$ is the radius of curvature of $B$. Then $\gamma_0 = (1 - \beta_0^2)^{-1/2} \approx (\omega/3c)^{1/3}$. Vacuum curvature emission maximizes for $\theta \approx 1/\gamma_0$. After putting in the sum over species explicitly into equation (86), we find

$$1 - \eta\beta_0 \cos\theta \approx \frac{1}{\gamma_0^2}\left[1 - \frac{1}{8}\frac{\epsilon}{\gamma_0^2}\left(\frac{r}{R_L}\right)^3\right], \tag{89}$$

where $\epsilon$ is the ratio of the energy density in accelerated particles (which have $u_m \gg \gamma_0$) to the magnetic energy density at the surface, a ratio equal to the fraction of the polar cap potential expended in creating the pair plasma. As a typical example in which $\epsilon$ is as small as possible, we use the space charge-limited beam model (Arons 1983*b*, eq. [84]). Then for the flow regions far from the slot gap,

$$\epsilon \approx 0.54\left(\frac{10^{12}\ \text{gauss}}{B_{\rm surface}}\right)P^{3/2} , \tag{90}$$

while $\gamma_0 \approx 50$–$100$ is typical for the emission of curvature photons at meter wavelengths. Vacuum curvature emission requires $r/R_L \ll 50(B_{\rm surface}/10^{12}\ \text{gauss})^{1/3}P^{-1/2}(100/\gamma_0)^{2/3}$.

For plasmas with energy as low as is implied by equation (90), therefore, Razin suppression is not a factor in bunched coherent curvature emission models, for radiation traveling almost parallel to the plasma. This conclusion assumes that the bunches correspond to small-amplitude disturbances in an otherwise weakly inhomogeneous plasma; if, instead, some unidentified mechanism can turn the plasma into small clouds propagating through a much more rarefied medium, our model of the plasma is inapplicable. While such a cloud model is unlikely (Ginzburg and Zheleznayakov 1975), it is not forbidden by any fundamental principle in a plasma where relative streaming between components can derive the formation of charge density fluctuations. More importantly, our estimates indicate the importance of taking the plasma into account self-consistently in analyzing the emission physics of any plasma model. Other possibilities for pulsar emission exist, of course, many of which do take the plasma into proper account from the beginning; see Michel (1982) and Lominadze and Pataraya (1982) for at least a mention of these.

### *b*) *Summary*

We have derived the complete dispersion relation for electromagnetic waves in ultrarelativistic, one-dimensional plasma in a very strong magnetic field including allowance for nonzero charge and field aligned current density (§ II). We extracted useful results for the dispersion relations when the two polarization states are approximately decoupled, as they should be in normal electron-positron plasmas in radio pulsars (§§ III, IV). We derived the Landau absorption rate for subluminous waves with Alfvén polarization in § V and used it to constrain the emission of such waves to radii small compared to the light cylinder, in the context of outflow of relativistic $e^{\pm}$ plasma along the polar field lines. We used our results to show how propagation effects can affect the emission physics, in the case of bunched coherent curvature radiation emitted by small-amplitude bunches propagating in a weakly inhomogeneous plasma (§ VI*a*). Our results are applied to the refraction of radio waves in the polar flow zones of pulsars in an accompanying paper; further applications of the basic dispersion relation (eq. [38]) will be discussed elsewhere.

Our research on this topic was supported by NSF grants AST 79-23243, AST 82-15456, and AST 83-17462, by grant number 85-6 from the Institute of Geophysics and Planetary Physics, and by the taxpayers of California.

REFERENCES

Aaron, R., and Currie, D. 1966, *Phys. Fluids*, **9**, 1423.
Arons, J. 1979, *Space Sci. Rev.*, **24**, 437.
———. 1981*a*, *Ap. J.*, **248**, 1099.
———. 1981*b*, in *Proc. Internat. Summer School and Workshop on Plasma Astrophysics*, ed. T. D. Guyenne (Paris: European Space Agency), p. 273.
———. 1983*a*, *Ap. J.*, **266**, 215.
———. 1983*b*, in *Electron-Positron Pairs in Astrophysics*, ed. M. L. Burns, A. K. Harding, and R. Ramaty (New York: American Institute of Physics), p. 163.
———. 1984, in *Advances in Space Research*, Vol. 3, ed. G. Bignami (London: Pergamon), p. 287.
Arons, J., Burnard, D. B., Klein, R. I., McKee, C. F., Pudritz, R., and Lea, S. M. 1984, in *High Energy Transients in Astrophysics*, ed. S. E. Woosley (New York: American Institute of Physics), p. 215.
———. 1986, *Ap. J.*, submitted.
Arons, J., and Lea, S. M. 1980, *Ap. J.*, **235**, 1016.
Arons, J., McKee, C. F., and Pudritz, R. 1985, *Ap. J.*, submitted.
Arons, J., and Scharlemann, E. T. 1979, *Ap. J.*, **231**, 854.
Asseo, E., Pellat, R., and Sol, H. 1983, *Ap. J.*, **266**, 201.
Baan, W., and Treves, A. 1973, *Astr. Ap.*, **21**, 792.
Baldwin, D. E., Bernstein, I. B., and Weenink, M. P. H. 1969, *Adv. Plasma Phys.*, **3**, 1.
Barnard, J. J., and Arons, J. 1982, *Ap. J.* **254**, 713.
———. 1986, *Ap. J.*, **302**, 138 (Paper II).
Barnes, A. 1966, *Phys. Fluids*, **9**, 1483.
Barnes, A., and Scargle, J. D. 1973, *Ap. J.*, **184**, 251.
Benford, G. 1975, *Ap. J.*, **201**, 419.
Buschauer, R., and Benford, G. 1977, *M.N.R.A.S.*, **179**, 99.
Cheng, A. F., and Ruderman, M. A. 1977, *Ap. J.*, **212**, 800.
———. 1979, *Ap. J.*, **229**, 348.
———. 1980, *Ap. J.*, **235**, 576.
Cheng, A. F., Ruderman, M. A., and Sutherland, P. 1976, *Ap. J.*, **203**, 209.
Cordes, J. M., and Hankins, T. 1977, *Ap. J.*, **218**, 484.
Davidson, K., and Ostriker, J. P. 1973, *Ap. J.*, **179**, 585.
Dawson, J. M. 1961, *Phys. Fluids*, **4**, 869.
Ghosh, P., and Lamb, F. K. 1979*a*, *Ap. J.*, **232**, 259.
———. 1979*b*, *Ap. J.*, **232**, 277.
Ginzburg, V. L., and Zheleznyakov, V. V. 1975, *Ann. Rev. Astr. Ap.*, **13**, 511.
Goldreich, P., and Julian, W. H. 1969, *Ap. J.*, **157**, 869.
Gruber, D. E., *et al.* 1980, *Ap. J.* (*Letters*), **240**, L127.
Hardee, P. E. 1979, *Ap. J.*, **227**, 958.
Harding, A. K., and Tademaru, E. 1979, *Ap. J.*, **233**, 317.
Jones, P. B. 1979, *Ap. J.*, **228**, 536.
———. 1982, *M.N.R.A.S.*, **197**, 1103.

Kirk, J. 1980, *Plasma Phys.*, **22**, 639.
Lamb, F. K. 1984, in *High Energy Transients in Astrophysics*, ed. S. E. Woosley (New York: American Institute of Physics), p. 179.
Lamb, F. K., Pethick, C. J., and Pines, D. 1973, *Ap. J.*, **184**, 271.
Lominadze, J. G., and Pataraya, V. 1982, *Phys. Scripta*, **T2**, 215.
Lominadze, J. G., Machabelli, G. Z., and Usov, V. V. 1983, *Ap. Space Sci.*, **90**, 19.
Mason, K. 1977, *M.N.R.A.S.*, **178**, 818.
Melrose, D. B. 1979, *Australian J. Phys.*, **32**, 61.
Melrose, D. B., and Stoneham, R. J. 1976, *Nuovo Cimento A*, **32**, 435.
———. 1977, *Proc. Astr. Soc. Australia*, **3**, 120.
Mészáros, P. 1984, in *High Energy Transients in Astrophysics*, ed. S. E. Woosley (New York: American Institute of Physics), p. 165.
Michel, F. C. 1982, *Rev. Mod. Phys.*, **54**, 1.
Onischenko, O. G. 1981, *Soviet Astr. Letters*, **7**, 404.
Ostriker, J. P., and Gunn, J. E. 1969, *Ap. J.*, **157**, 1395.
Pringle, J. E., and Rees, M. J. 1972, *Astr. Ap.*, **21**, 1.
Rappaport, S., and Joss, P. C. 1977, *Nature*, **266**, 683.
Ruderman, M. A., and Sutherland, P. G. 1975, *Ap. J.*, **196**, 51.
Stinebring, D. R., Cordes, J. M., Rankin, J. M., Weisberg, J. M., and Boriakoff, V. 1984*a*, *Ap. J. Suppl.*, **55**, 247.
———. 1984*b*, *Ap. J. Suppl.*, **56**, 279.
Sturrock, P. A. 1971, *Ap. J.*, **164**, 529.
Tademaru, E. 1973, *Ap. J.*, **183**, 623.
Tsytovitch, V. N., and Kaplan, S. A. 1972, *Astrofizika*, **8**, 441 (English transl. in *Astrophysics*, **8**, 260 [1972]).
Trumper, J., Pietsch, W., Reppin, C., Voges, W., Staubert, R., and Kendziorra, E. 1978, *Ap. J. (Letters)*, **219**, L105.
Voges, W., Pietsch, W., Reppin, C., Trumper, J., Kendziorra, E., and Staubert, R. 1982, *Ap. J.*, **263**, 803.

J. Arons: Department of Astronomy, 601 Campbell Hall, University of California, Berkeley, CA 94720

J. J. Barnard: Laboratory for High Energy Astrophysics, Code 665 NASA-Goddard Space Flight Center, Greenbelt, MD 20771